AD-A080 093 MISSISSIPPI STATE UNIV MISSISSIPPI STATE ENGINEERING--ETC F/G 20/4
NUMERICAL SOLUTION OF THE TWO-DIMENSIONAL INCOMPRESSIBLE AVERAG--ETC(U)
NOV 79 Z U WARSI, B B AMLICKE, J F THOMPSON AFOSR-76-2922

UNCLASSIFIED MSSU-EIRS-ASE-79-1 AFOSR-TR-80-0083 NL

| OF |
AD A
080093

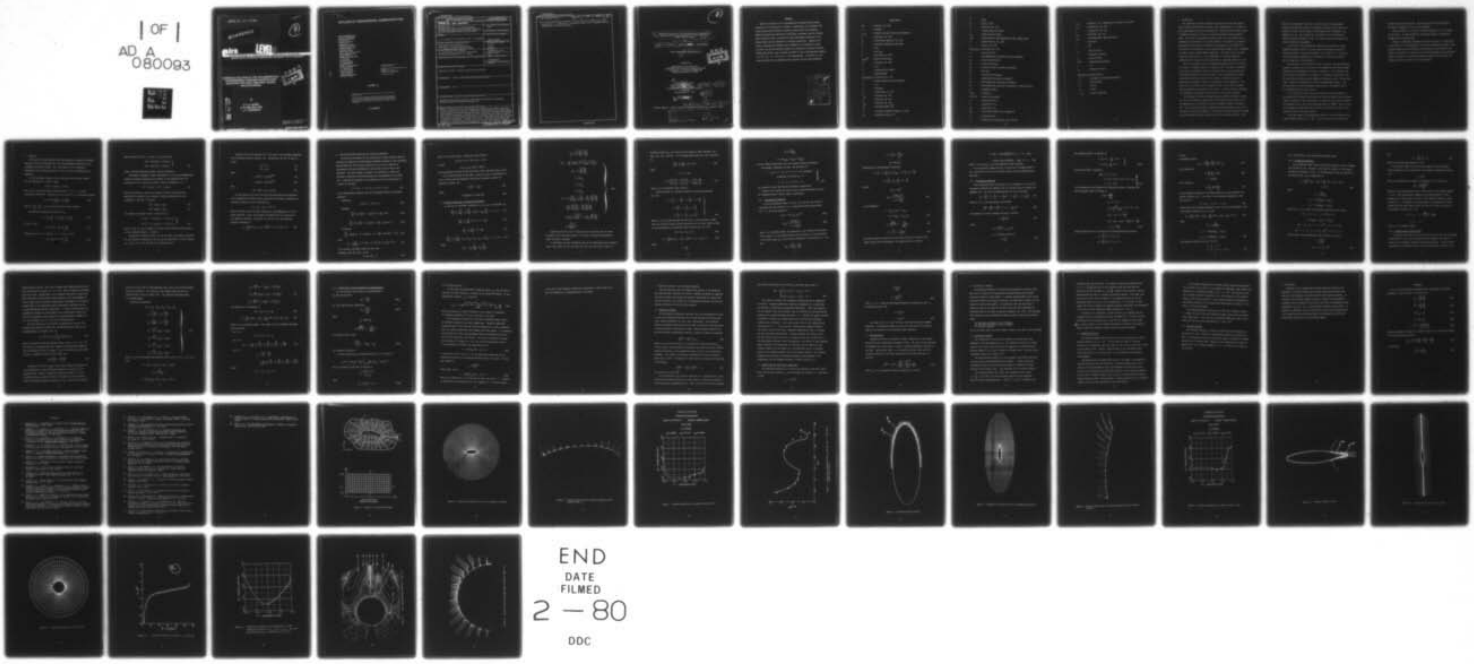

END
DATE
FILMED
2 — 80
DDC

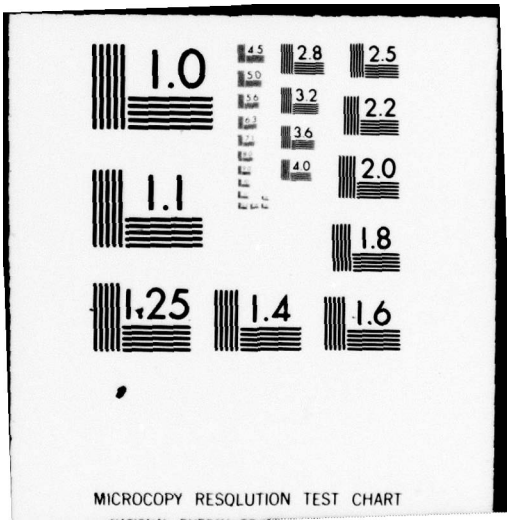
1.0
1.1
1.25
1.4
1.6
1.8
2.0
2.2
2.5
2.8
3.2
3.6
4.0
4.5
5.0
MICROCOPY RESOLUTION TEST CHART

(4)

eirs LEVEL II

ENGINEERING & INDUSTRIAL RESEARCH STATION

AEROPHYSICS & AEROSPACE ENGINEERING—MISSISSIPPI STATE UNIVERSITY

NUMERICAL SOLUTION OF THE TWO-DIMENSIONAL INCOMPRESSIBLE AVERAGED NAVIER-STOKES EQUATIONS FOR FINITE ARBITRARY SHAPED ISOLATED BODIES

by

Z. U. A. WARSI,
B. B. AMLICKE, AND
J. F. THOMPSON

Final Report-Part I

MSSU-EIRS-ASE-79-1

COLLEGE OF ENGINEERING ADMINISTRATION

WILLIE L. MCDANIEL, PH.D.
DEAN, COLLEGE OF ENGINEERING

WALTER R. CARNES, PH.D.
ASSOCIATE DEAN

RALPH E. POWE, PH.D.
ASSOCIATE DEAN

LAWRENCE J. HILL, M.S.
DIRECTOR, ENGINEERING EXTENSION

CHARLES B. CLIETT, M.S.
AEROSPACE ENGINEERING

WILLIAM R. FOX, PH.D.
AGRICULTURAL & BIOLOGICAL ENGINEERING

JOHN L. WEEKS, JR., PH.D.
CHEMICAL ENGINEERING

ROBERT M. SCHOLTES, PH.D.
CIVIL ENGINEERING

B. J. BALL, PH.D.
ELECTRICAL ENGINEERING

W. H. EUBANKS, M.ED.
ENGINEERING GRAPHICS

FRANK E. COTTON, JR., PH.D.
INDUSTRIAL ENGINEERING

C. T. CARLEY, PH.D.
MECHANICAL ENGINEERING

JOHN I. PAULK, PH.D.
NUCLEAR ENGINEERING

ELDRED W. HOUGH, PH.D.
PETROLEUM ENGINEERING

For additional copies or information
address correspondence to:

ENGINEERING AND INDUSTRIAL RESEARCH STATION
DRAWER DE
MISSISSIPPI STATE UNIVERSITY
MISSISSIPPI STATE, MISSISSIPPI 39762

TELEPHONE (601) 325-2266

UNCLASSIFIED

SECURITY CLASSIFICATION OF THIS PAGE (When Data Entered)

REPORT DOCUMENTATION PAGE	READ INSTRUCTIONS BEFORE COMPLETING FORM
1. REPORT NUMBER: AFOSR-TR- 80-0083	2. GOVT ACCESSION NO. / 3. RECIPIENT'S CATALOG NUMBER
4. TITLE (and Subtitle): NUMERICAL SOLUTION OF THE TWO-DIMENSIONAL IMCOMPRESSIBLE AVERAGED NAVIER-STOKES EQUATIONS FOR FINITE-ARBITRARY SHAPED ISOLATED BODIES PART I	5. TYPE OF REPORT & PERIOD COVERED: Final
	6. PERFORMING ORG. REPORT NUMBER
7. AUTHOR(s): Z. U. A. Warsi, B. B. Amlicke, and J. F. Thompson	8. CONTRACT OR GRANT NUMBER(s): AFOSR 76-2922
9. PERFORMING ORGANIZATION NAME AND ADDRESS: Mississippi State University, Department of Aerospace Engineering, P. O. Drawer A; Miss. State, MS 39762	10. PROGRAM ELEMENT, PROJECT, TASK AREA & WORK UNIT NUMBERS: 61102F, 2304/A3
11. CONTROLLING OFFICE NAME AND ADDRESS: Air Force Office of Scientific Research/NM, Bolling AFB, Washington, D.C. 20332	12. REPORT DATE: November 30, 1979
	13. NUMBER OF PAGES: 57
14. MONITORING AGENCY NAME & ADDRESS(if different from Controlling Office)	15. SECURITY CLASS. (of this report): UNCLASSIFIED
	15a. DECLASSIFICATION/DOWNGRADING SCHEDULE

16. DISTRIBUTION STATEMENT (of this Report)

Approved for public release; distribution unlimited

17. DISTRIBUTION STATEMENT (of the abstract entered in Block 20, if different from Report)

18. SUPPLEMENTARY NOTES

19. KEY WORDS (Continue on reverse side if necessary and identify by block number)

Averaged Navier-Stokes Solutions, Turbulence, Curvilinear Coordinates, Numerical Methods, Turbulence Modeling, etc.

20. ABSTRACT (Continue on reverse side if necessary and identify by block number)

Numerical solutions of the two-dimensional averaged Navier-Stokes equations for the prediction of laminar, transitional, and turbulent flow fields around finite bodies of arbitrary shapes have been considered. Numerically generated body-fitted curvilinear coordinates and the relevant metric terms are used to provide the finite-difference solutions of the Navier-Stokes and the equations of turbulent quantities. Complete flow fields, including the boundary layer parameters, are obtained by using the zero, one and two-equations models for Schubauer's elliptical section, NACA66$_3$-018 airfoil, and a circular cylinder

DD FORM 1473

Unclassified

20. Abstract Con't.

at free stream Reynolds numbers of 1.59 x 10^5, 1.2 x 10^6 and 1.4 x 10^6 respectively. In addition, a two-equation model with an algebraic-stress closure has also been developed.

(4)

(6) Numerical Solution of the Two-Dimensional Incompressible Averaged Navier-Stokes Equations for Finite Arbitrary Shaped Isolated Bodies, Part 1.

By

(10) Z. U. A. Warsi, B. B. Amlicke[redacted] J. F. Thompson

Report Number MSSU-EIRS-ASE-79-1
(14)

Prepared By

Mississippi State University
Engineering and Industrial Research Station
Department of Aerospace Engineering
Mississippi State, MS 39762

(9) Final Report, Part I
Under Grant
(15) AFOSR [redacted]-76-2922
(16) 2304
(17) A3
Air Force Office of Scientific Research
AFOSR/NM
Bolling AFB, DC 20332
(12) 57
(11) Nov[redacted]79
(19)
(18) AFOSR/TR-80-0083

*Present Address: Mission Research Corporation, Alexandria, Virginia 22312

390182

Abstract

Numerical solutions of the two-dimensional averaged Navier-Stokes equations for the prediction of laminar, transitional, and turbulent flow fields around finite bodies of arbitrary shapes have been considered. Numerically generated body-fitted curvilinear coordinates and the relevant metric terms are used to provide the finite-difference solutions of the Navier-Stokes and the equations of turbulent quantities. Complete flow fields, including the boundary layer parameters, are obtained by using the zero, one and two-equations models for Schubauer's elliptical section, $NACA66_3$-018 airfoil, and a circular cylinder at free stream Reynolds numbers of 1.59×10^5, 1.2×10^6 and 1.4×10^6 respectively. In addition, a two-equation model with an algebraic-stress closure has also been developed.

Nomenclature

A, B = Function, Eq. (48)

C = Constant

c_p, c_f = Pressure and Skin Friction Coefficients

D = Diffusion, Eq. (43)

D^2 = Differential Operator, Eq. (1b)

$\bar{e}$ = Turbulence Energy per Unit Mass

E = $\bar{e}/u_\infty^2$

g = det (g_{ij})

G = Function, Eq. (40d)

g_{ij}, g^{ij} = Metric Coefficients

H = Function, Eq. (40c)

k = 0.41

L = Characteristic Length

ℓ = Mixing Length

M_1, M_2, N_1, N_2 = Functions, Eq. (53)

n = Normal Distance from the Surface

N = n/L

p = Pressure

P = Production, Eq. (38)

P_{ij} = Function, Eq. (25)

Q = Function, Eq. (34)

Q_{ij} = Function, Eq. (25)

R_o = Reynolds Number $\frac{U_\infty L}{\nu}$

R = Turbulence Reynolds Number, Eq. (40)

R_r = Reference Value of R

$\hat{R}$ = R/R_r

R_ω = $R_o/(1 + R_oT)$

S = Function, Eq. (25)

s = Length Along the Surface

S_{ij} = Rate-of-Strain Tensor

t_1, t = Dimensional and Non-Dimensional Times, Respectively

T = Eddy Viscosity, Eq. (28)

$\underset{\sim}{T}$ = Vector, Eq. (18)

T_1, T_2, T_3, T_4 = Functions, Eq. (53)

$\underset{\sim}{u}$ = Velocity Vector

u,v = Non-Dimensional Cartesian Velocity Components

u_∞ = Free Stream Velocity

U_* = Friction Velocity

U_s = Velocity Along the Surface Coordinates

U_p = Max (U_s)

W = Acceleration Parameter

x_i = Subscripted Cartesian Coordinates

x,y = Non-Dimensional Cartesian Coordinates

y_i = Non-Dimensional Cartesian Coordinates in Subscript Form

Z_r = Roughness Height

α_o, β_1 = Constants

$\xi^1=\xi, \xi^2=\eta$ = General Coordinates

ϕ = General Function

∇^2 = Laplacian in x,y

∇_1^2 = Laplacian in x_i

Γ^r_{ij} = Christoffel Symbol, (see Appendix A)

ψ = Stream Function

τ, σ = Geometrical Coefficients, Eqs. (9),(10)

τ_1, σ_1 = Modified τ and σ Respectively, Defined in the Text

ε_{ij} = Dissipation, Eq. (25)

χ = Dissipation, Eq. (42)

Δ_{ij} = Diffusion, Eq. (25)

τ_{ij} = Non-Dimensional Reynolds Stress

ω = Vorticity

Ω = $\frac{\omega}{R_\omega}$

ω_w = Wall Vorticity

ν = Kinematic Viscosity

ν_T = Eddy Viscosity

δ^*, Δ^* = Displacement Thickness

Λ = ℓ/L

γ_{tr} = Transition Factor

Subscripts and Superscripts:

$(\bar{.})$ = Averaged and Dimensional Quantity

$(.)'$ = Perturbation

$(\tilde{:})$ = Tensor

$(\underset{\sim}{.})$ = Vector

$(.)_{ij}$ = Tensor Components

1. Introduction

The computation of mean turbulent flow fields for flows past finite bodies without effecting the thin shear layer approximation is a problem of much computational and practical importance. There are three distinct areas of immediate attention if one is to solve the problem of mean turbulent flows. The first is the problem of and the order of closure which can be considered as satisfactory for a given problem. The second is in regard to the generality and ease with which the body geometry can be brought into the process of calculations so that arbitrary shaped bodies can be considered as simply as those having simpler geometries. The third, and by no means lesser than the above two, is the development of efficient numerical techniques which can give accurate solutions in reasonable amounts of time.

Most of our present state of knowledge regarding closure is usually in the context of boundary layers, far wakes and jets. Not much is available by the way of experimental data for turbulent flows in the separated and recirculating regions near a body surface. Thus the modeling of various terms which have proved useful in the context of boundary layers are heuristically extended to apply for non-boundary layer regions too. How much error is introduced in the predicted values of the field variables this way remains to be checked in the future. A recent article by Reynolds [1] summarizes the present state-of-the-art in the closure problem.

The problem of arbitrary shaped bodies and general coordinate systems for use in the numerical computations of the viscous flow problems is not as compelling as it was before the work of Thompson, Thames, and Mastin [2]. The so called body-fitted coordinates method developed in Ref. [2] is the method in which the geometry of the body is entirely preserved by taking the curve forming the body surface as one of the coordinate curves. This

method has successfully been used in solving various fluid dynamical problems including the problem of supersonic flow past a blunt body, [3]. Though at present various authors are developing other techniques, e.g., Shamroth, et. al., [4], Eiseman [5], and Davis [6], the "differential equation" approach initiated in Ref. [2] looks to have more potential for future research and development.

In the area of finite-difference method for the solution of fluid dynamical equations there are various explicit and implicit methods of solution available in the open literature, e.g., Roache [7]. The choice of a method usually depends on the formulation of the overall problem and the character of the equations.

The main aim of this research has been to develop a suitable numerical program of solution for the solution of two-dimensional mean Navier-Stokes equations in non-orthogonal curvilinear coordinates. The coordinates and all the metric coefficients are assumed to be available in numerical form. The body-fitted coordinate system generation technique of Ref. [2] has been used to generate coordinates for various two-dimensional shapes. Care has been taken to have the maximum concentration of coordinate lines in the neighborhood of the body surface.

In the present research three body shapes have been considered for the prediction of laminar transitional and turbulent regions using different orders of modeling. The first-shape is an elliptical section as considered by Schubauer [8] at a free stream Reynolds number of 158860. Both the zero- and one-equation models have been used with the transitional model at the predicted points on the body surface.

The second shape is the $NACA66_3$-018 airfoil at zero incidence and the chord Reynolds number of 1.2×10^6. In this case also the zero-and one-

equation models have been used. The energy equation has been modeled according to Glushko [9] in both these problems.

The third shape is a circle at a Reynolds number of 1.4×10^6 based on the radius. In this problem the two-equations model of Saffman and Kolmogorov [10] has been used.

Details of turbulence modelings are given in Section 3 of this paper. In the course of our investigation, we have also developed a method of two-equations model with the Reynolds stress algebraic closure which can be called as equivalent to solving all the relevant Reynolds stress equations. However, because of the storage requirements needed by this method, the method could not be tested for all the problems.

2. Analysis

This section briefly describes the basic aspects of numerical coordinate generation and the transformation of the fluid dynamical equations to non-orthogonal coordinate systems. For a description of the quantities appearing in the following equations, refer to the list of symbols and to Appendix A.

All the pertinent formulae used in this paper stem from the formula for the Laplacian of a scalar ϕ, where

$$\phi(x,y) = \phi(x(\xi,\eta),\ y(\xi,\eta)).$$

Here x and y are the Cartesian coordinates and $\xi^1 = \xi$, $\xi^2 = \eta$ are the curvilinear coordinates. The Laplacian $\nabla^2\phi$ in the (ξ^1,ξ^2) coordinates becomes

$$\nabla^2\phi = g^{ij}\left(\frac{\partial^2\phi}{\partial\xi^i\,\partial\xi^j} - \Gamma^r_{ij}\,\frac{\partial\phi}{\partial\xi^r}\right) \tag{1a}$$

where $\nabla^2 = \dfrac{\partial^2}{\partial x^2} + \dfrac{\partial^2}{\partial y^2}$, and the repeated indices imply summation.

Introducing a differential operator D^2 as

$$D^2 \equiv g_{22}\,\frac{\partial^2}{\partial\xi^2} - 2g_{12}\,\frac{\partial^2}{\partial\xi\,\partial\eta} + g_{11}\,\frac{\partial^2}{\partial\eta^2} \tag{1b}$$

in (1a), we get

$$\nabla^2\phi = \frac{1}{g}\,D^2\phi - g^{ij}\,\Gamma^r_{ij}\,\frac{\partial\phi}{\partial\xi^r} \tag{1c}$$

Setting in turn $\phi = \xi^1 = \xi$ and $\phi = \xi^2 = \eta$ in (1c), we get

$$\nabla^2\phi = \frac{1}{g}\,D^2\phi + (\nabla^2\xi^r)\,\frac{\partial\phi}{\partial\xi^r} \tag{1d}$$

Again setting in turn $\phi = x$ and $\phi = y$ in (1d), we get

$$\left.\begin{aligned} D^2x &= -g[(\nabla^2\xi)x_\xi + (\nabla^2\eta)x_\eta] \\ D^2y &= -g[(\nabla^2\xi)y_\xi + (\nabla^2\eta)y_\eta] \end{aligned}\right\} \qquad (2)$$

where a variable subscript denotes a partial derivative.

The method of Thompson, Thames, and Mastin [2] for the two-dimensional numerical coordinate generation now depends on the assumption that the coordinates ξ and η satisfy an elliptic system of equations, i.e.,

$$\nabla^2\xi = -f_1(\xi,\eta) \ , \ \nabla^2\eta = -f_2(\xi,\eta) \ , \qquad (3)$$

where the functions f_1 and f_2 are treated as control functions to be specified in a manner so as to achieve a desired distribution of the coordinates. Thus Eqs. (2) become

$$D^2x = g(f_1x_\xi + f_2x_\eta) \qquad (4)$$

$$D^2y = g(f_1y_\xi + f_2y_\eta) \qquad (5)$$

The boundary conditions for Eqs. (4) and (5) are

$$\left.\begin{aligned} &\text{on } \Gamma_1^*: \quad x = F_1(\xi,\eta_B) \ , \ y = F_2(\xi,\eta_B) \\ &\text{on } \Gamma_2^*: \quad x = G_1(\xi,\eta_\infty) \ , \ y = G_2(\xi,\eta_\infty) \end{aligned}\right\} \qquad (6)$$

where Γ_1^* and Γ_2^* are the images of the body and the external body contours in the transformed plane, cf. Figure 1.

The method of solution of Eqs. (4) and (5) under the boundary conditions (6) with periodic conditions on the cut has been described in various reports, e.g., [11], [12], [13], and will not be described here.

Another form of the Laplacian $\nabla^2\phi$, to be used in the transport equations, can be obtained directly from Eqs. (2). Solving Eqs. (2) for $\nabla^2\xi$ and $\nabla^2\eta$, we get

$$\nabla^2\xi = \tau/g \tag{7}$$

$$\nabla^2\eta = \sigma/g \tag{8}$$

where

$$\tau = (x_\eta D^2 y - y_\eta D^2 x)/g^{1/2} \tag{9}$$

$$\sigma = (y_\xi D^2 x - x_\xi D^2 y)/g^{1/2} \tag{10}$$

Thus

$$\nabla^2\phi = (D^2\phi + \tau\phi_\xi + \sigma\phi_\eta)/g \tag{11}$$

In this paper we have used the vorticity-stream function formulation for the equations of motion, which, along with the transport equations for turbulence quantities can be represented as

$$\lambda_t + \psi_y\lambda_x - \psi_x\lambda_y = \nabla^2\bar{\lambda} + B$$

where all quantities in the above equation are non-dimensional; ψ is the stream function, λ and $\bar{\lambda}$ are surrogate variables and B is a function of the dependent variables. Using Eqs. (7) and (8), the representative equation transforms as

$$\lambda_t + \frac{1}{g^{1/2}}(\psi_\eta\lambda_\xi - \psi_\xi\lambda_\eta) = \frac{1}{g}(D^2\bar{\lambda} + \tau\bar{\lambda}_\xi + \sigma\bar{\lambda}_\eta) + B\ . \tag{12}$$

3. Mean Navier-Stokes Equations and Turbulence Modeling

The pertinent equations for the description of mean turbulent flow are obtained by replacing the instantaneous dependent variables in the continuity, Navier-Stokes and the vorticity equations by the sum of a mean and a perturbation and then performing the time average of each term of the equations. The time average is assumed to be performed to remove the turbulent fluctuations while maintaining the time dependency of the mean flow. Denoting the averages by an overhead bar and the fluctuations by a prime, we introduce

$$\underset{\sim}{u} = \bar{\underset{\sim}{u}} + \underset{\sim}{u}' \ , \ p = \bar{p} + p' , \ \underset{\sim}{\omega} = \bar{\underset{\sim}{\omega}} + \underset{\sim}{\omega}' , \text{ etc.} \tag{13}$$

in the instantaneous equations and after averaging obtain the following equations.

Continuity:

$$\operatorname{div} \bar{\underset{\sim}{u}} = o \ , \ \operatorname{div} \bar{\underset{\sim}{\omega}} = o \tag{14}$$

Momentum:

$$\frac{\partial \underset{\sim}{u}}{\partial t_1} + \operatorname{div} (\bar{\underset{\sim}{u}}\bar{\underset{\sim}{u}}) = - \frac{1}{\rho} \operatorname{grad} \bar{p} + \nu \nabla_1^2 \bar{\underset{\sim}{u}} - \operatorname{div} \bar{\underset{\approx}{\tau}} \tag{15a}$$

$$\frac{\partial \bar{\underset{\sim}{u}}}{\partial t_1} + \operatorname{div} (\bar{\underset{\sim}{u}}\bar{\underset{\sim}{u}}) = - \frac{1}{\rho} \operatorname{grad} \bar{p} + \nu \nabla_1^2 \bar{\underset{\sim}{u}} - \operatorname{grad} \bar{e} + \underset{\sim}{T} \tag{15b}$$

Vorticity:

$$\frac{\partial \bar{\underset{\sim}{\omega}}}{\partial t_1} + (\operatorname{grad} \bar{\underset{\sim}{\omega}}) \cdot \bar{\underset{\sim}{u}} - (\operatorname{grad} \bar{\underset{\sim}{u}}) \cdot \bar{\underset{\sim}{\omega}} = \nu \nabla_1^2 \bar{\underset{\sim}{\omega}} + \operatorname{div} (\overline{\underset{\sim}{u}'\underset{\sim}{\omega}'} - \overline{\underset{\sim}{\omega}'\underset{\sim}{u}'}) \tag{16}$$

where

$$\nabla_1^2 = \frac{\partial^2}{\partial x_i \partial x_j} \ , \ \bar{\underset{\approx}{\tau}} = \overline{\underset{\sim}{u}'\underset{\sim}{u}'} \ , \ \underset{\sim}{T} = \overline{\underset{\sim}{u}' \times \underset{\sim}{\omega}'} , \ \bar{e} = \frac{1}{2} \overline{\underset{\sim}{u}' \cdot \underset{\sim}{u}'} \ , \tag{17}$$

$\bar{e}$ is the mean turbulence energy per unit mass.

Comparing (15a) and (15b), we get

$$\underset{\sim}{T} = \operatorname{div} (\bar{e}\underset{\approx}{I} - \bar{\underset{\approx}{\tau}}) \ , \tag{18}$$

where $\tilde{I}$ is the unit tensor. Using the vector identity

$$\text{curl } (\underset{\sim}{u}' \times \underset{\sim}{\omega}') = \text{div } (\underset{\sim}{u}'\underset{\sim}{\omega}' - \underset{\sim}{\omega}'\underset{\sim}{u}')$$

we have

$$\text{curl } \underset{\sim}{T} = \text{div } (\overline{\underset{\sim}{u}'\underset{\sim}{\omega}'} - \overline{\underset{\sim}{\omega}'\underset{\sim}{u}'}) \ ,$$

which establishes the form of the last term on the right hand side of (16).

In all cases studied in this paper, except the one to be described in 3.1.4, we have used the Newtonian constitutive equation to model the Reynolds stresses, viz.,

$$\tilde{\tau} = \frac{2}{3}\bar{e}\tilde{I} - 2\nu_T\tilde{D} \tag{19}$$

where

$$\tilde{D} = \frac{1}{2}[\text{grad } \underset{\sim}{\bar{u}} + (\text{grad } \underset{\sim}{\bar{u}})^*] \tag{20}$$

3.1 Transport Equations in Cartesian Coordinates

In the case of Cartesian coordinates, x_1, x_2, x_3, the equations are

$$\frac{\partial\bar{\omega}_i}{\partial t_1} + \bar{u}_k\frac{\partial\bar{\omega}_i}{\partial x_k} - \bar{\omega}_k\frac{\partial\bar{u}_i}{\partial x_k} = \nu\nabla_1^2\omega_i + e_{ijk}\frac{\partial T_k}{\partial x_j} \ , \ i = 1,2,3 \tag{21}$$

$$\frac{\partial\bar{e}}{\partial t_1} + \bar{u}_k\frac{\partial\bar{e}}{\partial x_k} = \bar{P} + \bar{D} - \bar{\varepsilon} + \nu\nabla_1^2\bar{e} \tag{22}$$

$$\frac{\partial\bar{\varepsilon}}{\partial t_1} + \bar{u}_k\frac{\partial\bar{\varepsilon}}{\partial x_k} = \bar{S} + \nu\nabla_1^2\bar{\varepsilon} \tag{23}$$

$$\frac{\partial\bar{\tau}_{ij}}{\partial t_1} + \bar{u}_k\frac{\partial\bar{\tau}_{ij}}{\partial x_k} = \bar{P}_{ij} + \bar{Q}_{ij} + \bar{\Delta}_{ij} - \bar{\varepsilon}_{ij} + \nu\nabla_1^2\bar{\tau}_{ij} \ , \ i,j = 1,2,3 \ . \tag{24}$$

where

$$\bar{P}_{ij} = -(\bar{\tau}_{ik}\frac{\partial\bar{u}_j}{\partial x_k} + \bar{\tau}_{jk}\frac{\partial\bar{u}_i}{\partial x_k})$$

$$\bar{Q}_{ij} = \overline{\frac{p'}{\rho}\left(\frac{\partial u_i'}{\partial x_j} + \frac{\partial u_j'}{\partial x_i}\right)}$$

$$\bar{\Delta}_{ij} = -\frac{\partial}{\partial x_k}\left[\overline{\tau_{ij}u_k'} + \overline{\frac{p'}{\rho}\left(u_j'\delta_{ik} + u_i'\delta_{jk}\right)}\right]$$

$$\bar{\varepsilon}_{ij} = 2\nu\,\overline{\frac{\partial u_i'}{\partial x_k}\frac{\partial u_j'}{\partial x_k}}$$

$$\bar{P} = \frac{1}{2}\bar{P}_{ii}$$

$$\bar{D} = \frac{1}{2}\bar{\Delta}_{ii}$$

$$\bar{\varepsilon} = \frac{1}{2}\bar{\varepsilon}_{ii}$$

$$\bar{S} = -2\nu\left[\frac{\partial^2\bar{u}_j}{\partial x_\ell \partial x_k}\overline{\left(u_k'\frac{\partial u_j'}{\partial x_\ell}\right)} + \frac{\partial\bar{u}_j}{\partial x_k}\overline{\left(\frac{\partial u_j'}{\partial x_\ell}\frac{\partial u_k'}{\partial x_\ell}\right)}\right.$$

$$+ \frac{\partial\bar{u}_k}{\partial x_\ell}\overline{\left(\frac{\partial u_j'}{\partial x_\ell}\frac{\partial u_j'}{\partial x_k}\right)} + \overline{\frac{\partial u_j'}{\partial x_\ell}\frac{\partial u_j'}{\partial x_k}\frac{\partial u_k'}{\partial x_\ell}}$$

$$+ \frac{1}{2}\frac{\partial}{\partial x_k}\overline{\left(u_k'\left(\frac{\partial u_j'}{\partial x_\ell}\right)^2\right)} + \frac{1}{\rho}\frac{\partial}{\partial x_j}\overline{\left(\frac{\partial u_j'}{\partial x_\ell}\frac{\partial p'}{\partial x_\ell}\right)}$$

$$\left. + \nu\overline{\left(\frac{\partial^2 u_j'}{\partial x_k \partial x_\ell}\right)^2}\right] \qquad (25)$$

Equations (21)-(25) form a closed system of equations when the terms occuring in (25) have been modeled on the basis of empirical-experimental and/or heuristic reasoning.

In this paper, we have considered only the two-dimensional mean turbulent flows, and, except for one case where Eq. (24) has been used to model the

Reynolds stresses $\bar{\tau}_{ij}$, all cases use the concept of eddy viscosity, viz., Eqs. (19), (22), and (23). For two-dimensional flows, Eq. (21) is written as

$$\frac{\partial \bar{\omega}}{\partial t_1} + \bar{u}_k \frac{\partial \bar{\omega}}{\partial x_k} = \nabla_1^2 \bar{\Omega} + \bar{B} \tag{26}$$

where

$$\bar{\Omega} = (\nu + \nu_T)\bar{\omega}$$

$$\bar{B} = 2\left(\frac{\partial^2 \nu_T}{\partial x_1^2} \frac{\partial \bar{u}_1}{\partial x_2} - \frac{\partial^2 \nu_T}{\partial x_2^2} \frac{\partial \bar{u}_2}{\partial x_1} + 2 \frac{\partial^2 \nu_T}{\partial x_1 \partial x_2} \frac{\partial \bar{u}_2}{\partial x_2}\right) \tag{27}$$

where ν_T is the kinematic eddy viscosity.

We now introduce the following scheme for non-dimensionalizing Eq. (26):

$$\left.\begin{aligned} \Omega = \frac{\bar{\Omega}}{u_\infty^2}\ ,\ \omega = \frac{L\bar{\omega}}{u_\infty}\ ,\ T = \frac{\nu_T}{u_\infty L}\ ,\ \psi = \frac{\bar{\psi}}{u_\infty L} \\ t = \frac{u_\infty t_1}{L}\ ,\ u = \frac{\bar{u}_1}{u_\infty}\ ,\ v = \frac{\bar{u}_2}{u_\infty} \\ x = \frac{x_1}{L}\ ,\ y = \frac{y_1}{L}\ ,\ R_o = \frac{u_\infty L}{\nu} \end{aligned}\right\} \tag{28}$$

Where u_∞ is the freestream mean velocity and L a characteristic length. Thus the vorticity-stream function formulation for the flow field in terms of the non-dimensional coordinates takes the form (cf. Eq. (12))

$$D^2\psi + \tau\psi_\xi + \sigma\psi_\eta = -g\omega \tag{29}$$

$$\omega_t + \frac{1}{g^{1/2}}(\psi_\eta \omega_\xi - \psi_\xi \omega_\eta) = \frac{1}{g}(D^2\Omega + \tau\Omega_\xi + \sigma\omega_\eta) + B \tag{30}$$

where

$$\Omega = \frac{\omega}{R_\omega}$$

$$R_\omega = \frac{R_o}{1 + R_o T}$$

$$B = 2(T_{xx} u_y - T_{yy} v_x + 2T_{xy} v_y)$$

and the variable subscripts ξ, η, x and y denote partial derivatives.

The boundary conditions for Eqs. (29) and (30) are:

$$\left.\begin{aligned} \eta = \eta_B &: \psi = 0\ ,\ \psi_y = 0;\ T = 0;\ \omega \text{ to be calculated} \\ &\quad \text{iteratively to satisfy } \psi_y = 0\ . \\ \eta \to \eta_\infty &: \psi \to y;\ T \to 0;\ \omega \to 0\ , \end{aligned}\right\} \qquad (31)$$

η_B, η_∞ denote the wall and external boundaries respectively.

Below we now consider the zero, one and two-equation models and also the "algebraic-stress closure" model, respectively.

3.1.1 Zero-Equation Modeling

In the zero-equation model, only Eqs. (29) and (30) are solved by specifying the eddy viscosity ν_T by a generalized mixing length model (cf. [1], [14]) and defined as

$$(\nu_T)_i = \ell^2 (2\, \bar{S}_{ij}\, \bar{S}_{ij})^{1/2} \qquad (32a)$$

$$(\nu_T)_o = \frac{.0168 |\bar{u}_p| \delta^*}{1 + 5.5(\frac{n}{n_\delta})^6} \qquad (32b)$$

where ℓ is the mixing length, the subscripts i and o denote the inner and outer values, n is the normal distance from the body, n_δ is the thickness of the shear layer, $\bar{u}_p$ is the velocity tangential to the surface at $n = n_\delta$, and

$$\bar{S}_{ij} = \frac{1}{2}(\frac{\partial \bar{u}_i}{\partial x_j} + \frac{\partial \bar{u}_j}{\partial x_i})$$

$$\delta^* = \int_o^{n_\delta} (1 - \frac{\bar{u}_s}{\bar{u}_p}) dn$$

$$\bar{u}_p = \max (\bar{u}_s)$$

Introducing the non-dimensional quantities

$$\Lambda = \frac{\ell}{L} , \; Q = \frac{L^2}{u_\infty^2} (2 \bar{S}_{ij} \bar{S}_{ij}) , \; N = \frac{n}{L} , \; N_\delta = \frac{n_\delta}{L} ,$$

$$U_s = \frac{\bar{u}_s}{u_\infty} , \; U_p = \frac{\bar{u}_p}{u_\infty} , \; \Delta^* = \frac{\delta^*}{L}$$

We have

$$(T)_i = \Lambda^2 Q^{1/2}$$

$$(T)_o = \frac{.0168 |U_p| \Delta^*}{1 + 5.5 (\frac{N}{N_\delta})^6} \tag{33}$$

In two dimensions

$$Q = (\psi_{xx} - \psi_{yy})^2 + 4 \psi_{xy}$$

$$= \omega^2 + 4(\psi_{xy}^2 - \psi_{xx} \psi_{yy}) \tag{34}$$

$$U_s = \sqrt{\frac{g_{11}}{g}} \psi_\eta - \frac{g_{12}}{\sqrt{g g_{11}}} \psi_\xi \tag{35}$$

$$\Delta^* = \int_o^{N_\delta} (1 - \frac{U_s}{U_p}) dN \tag{35}$$

The mixing length is given by the Van Driest formula for the near wall region joined with the Bradshaw's [15] empirical fit as follows.

$$\Lambda = kN[1 - \exp(-N\sqrt{R_o|\omega_w|}/26\cdot)] \ , \ o < N < .22N_\delta$$

$$= .089N_\delta \tanh(4.6067N/N_\delta) \ , \ .22N_\delta < N < \infty \qquad (36)$$

where $k = 0.41$ and ω_w is the non-dimensional wall vorticity.

In the numerical computation $(T)_i$ is used till it becomes equal to $(T)_o$, and then for the rest of the shear layer the outer expression has been used.

3.1.2 One-Equation Modeling

The one-equation model is basically due to Glushko [9] in the form presented by Beckwith and Bushnell [16] and recently used by Coakley and Bergmann [14]. We first non-dimensionalize Eq. (22) as follows:

$$T_{ij} = \frac{\bar{\tau}_{ij}}{u_\infty^2} \ , \ E = \frac{\bar{e}}{u_\infty^2} \ , \ P = \frac{L}{u_\infty^3}\bar{P} \ , \ \chi = \frac{L}{u_\infty^3}\bar{\varepsilon} \ , \ D = \frac{L}{u_\infty^3}\bar{D} \qquad (37)$$

Thus Eq. (22) in non-dimensional form becomes

$$\frac{\partial E}{\partial t} + u\frac{\partial E}{\partial x} + v\frac{\partial E}{\partial y} = P + D - \chi + \frac{1}{R_o}\nabla^2 E \ . \qquad (38)$$

The modeling of various unknowns proceeds as follows:

$$T = \frac{\alpha R}{R_o} H(\hat{R}) \qquad (39)$$

where

$$R = \frac{(\bar{e})^{1/2}\ell}{\nu} = R_o \Lambda E^{1/2}$$

R_r = reference value of R

$$\hat{R} = \frac{R}{R_r} \qquad (40a)$$

The integral length Λ is defined as

$$\left.\begin{aligned} \Lambda = \frac{\ell}{L} &= N \ , \quad \frac{N}{N_\delta} < 0.2 \\ &= 0.2\, N_\delta \ , \ \frac{N}{N_\delta} > 0.2 \end{aligned}\right\} \tag{40b}$$

The function $H(\hat{R})$ is defined as

$$\left.\begin{aligned} H(\hat{R}) &= \hat{R} \ , \ \hat{R} < 0.75 \\ &= \hat{R} - (\hat{R} - 0.75)^2, \ 0.75 < \hat{R} < 1.25 \\ &= 1 \ , \ R > 1.25 \end{aligned}\right\} \tag{40c}$$

In the modeling of the diffusion and dissipation terms, a function $G(\hat{R})$ will be needed, which is defined as

$$\begin{aligned} G(\hat{R}) &= \frac{H(k\hat{R})}{H(\hat{R})} \\ &= k \ , \ \hat{R} < 0.75 \\ &= \frac{k\hat{R}}{\hat{R} - (\hat{R} - 0.75)^2} \ , \ 0.75 < \hat{R} < 1.25 \\ &= k\hat{R} \ , \ 1.25 < \hat{R} < \frac{0.75}{k} \\ &= k\hat{R} - (k\hat{R} - 0.75)^2 \ , \ \frac{0.75}{k} < \hat{R} < \frac{1.25}{k} \\ &= 1 \ , \ \hat{R} > \frac{1.25}{k} \end{aligned} \tag{40d}$$

Having defined H and G, and using the following abbreviated notation

$$y_i = \frac{x_i}{L} \ (y_1 = x, \ y_2 = y)$$

$$u_i = \frac{\bar{u}_i}{u_\infty} \ (u_1 = u, \ u_2 = v)$$

we have,

(i) Reynolds stress:

$$T_{ij} = -T\left(\frac{\partial u_i}{\partial y_j} + \frac{\partial u_j}{\partial y_i}\right) + \frac{2}{3} E \delta_{ij} \tag{41}$$

(ii) Dissipation:

$$\chi = \frac{cE}{\Lambda^2} \left(\frac{1}{R_o} + kGT\right) , \tag{42}$$

$$c = \text{constant} .$$

(iii) Diffusion:

$$D = \frac{\partial}{\partial y_k} \left(kGT \frac{\partial E}{\partial y_k}\right) \tag{43}$$

In the numerical solution of the energy equation, we have neglected the spatial variation of G. The values of the constants appearing in (39) and (42) are:

$$k = 0.41 , \alpha = 0.2 , c = 3.93 \tag{44}$$

Substituting the preceding expressions in Eq. (38) and transforming to the curvilinear coordinates (ξ,η), we have

$$E_t + \frac{1}{g^{1/2}} \left(\psi_\eta E_\xi - \psi_\xi E_\eta\right) = \frac{1}{gR_e} \left(D^2 E + \tau_1 E_\xi + \sigma_1 E_\eta\right) + TQ - \chi \tag{45}$$

where

$$R_e = \frac{R_o}{1 + kGR_o T}$$

$$\tau_1 = \tau + kGR_e\left(g_{22}T_\xi - g_{12}T_\eta\right)$$

$$\sigma_1 = \sigma + kGR_e\left(g_{11}T_\eta - g_{12}T_\xi\right) \tag{46}$$

The boundary conditions for Eq. (45) are:

$$\eta = \eta_B : \quad E = o$$

$$\eta \to \eta_\infty : \quad E \to o , \text{ or } E_\infty , \tag{47}$$

E_∞ is proportional to the freestream turbulence level.

3.1.3 Two-Equation Modeling

The two-equation model used in the present research is due to Saffman [10] and Wilcox [17]. Details of this model in relation to the present research are available in [18]. In non-dimensional form, any equation of the present model can be represented as

$$\lambda_t + \frac{1}{g^{1/2}} (\psi_\eta \lambda_\xi - \psi_\xi \lambda_\eta) = \frac{1}{gR_\lambda} (D^2\lambda + \tau_1 \lambda_\xi + \sigma_1 \lambda_\eta) + A\lambda + B \qquad (48)$$

where

$$R_\lambda = \frac{R_o}{1 + C_\lambda T}$$

$$\tau_1 = \tau + MR_\lambda (g_{22} T_\xi - g_{12} T_\eta)$$

$$\sigma_1 = \sigma + MR_\lambda (g_{11} T_\eta - g_{12} T_\xi)$$

The form of A, B, C_λ and M for different equations are as follows:

For $\lambda = \omega$: $C_\lambda = 2$, $A = 2\nabla^2 T$, $M = 4$,

$$B = 4(T_{xx} u_y - T_{yy} v_x + 2 T_{xy} v_y)$$

For $\lambda = E$: $C_\lambda = 1$, $A = -\phi^{1/2}$, $M = 1$, $B = 2TQ$

For $\lambda = \phi$: $C_\lambda = 1$, $A = P_1 - \beta_1 \phi^{1/2}$, $M = 1$, $B = o$

In this model the non-dimensional eddy viscosity is given by

$$T = \frac{\alpha_o{}^2 E}{2\phi^{1/2}}$$

$$\alpha_o = 0.3 \ , \ \beta_1 = 5/3 \qquad (49)$$

and

$$P_1 = \frac{\alpha_o^2}{8} (Q + \omega^2) \qquad (50)$$

where Q has already been defined in (34).

The function ϕ which has its own rate equation is the turbulence vorticity-density and is related with the turbulence dissipation function χ as

$$\chi \simeq E\phi^{1/2}$$

Thus in the turbulent core region, the behaviour of ϕ is such that

$$\phi^{1/2} = \frac{\alpha_o(\alpha_o E)^{1/2}}{kN}$$

where N is the normal distance from the wall and k is the Karman constant ($\simeq 0.41$). This consideration together with an approximation of the E equation near a wall yields the value of the empirical constant α_o which is nearly 0.3. Proceeding in the same manner, an approximation of the ϕ-equation near the wall region yields the value of β_1 which is nearly 5/3. The boundary conditions for ϕ are

$$\text{at } \eta = \eta_\beta : \quad \phi = \left(\frac{2500\ \alpha_o}{R_o}\right)^2 \left(\frac{L}{Z_r}\right)^4$$

$$\eta = \eta_\infty : \quad \phi \to o$$

where Z_r is a roughness length.

3.1.4 Algebraic-Stress Closure Model

It has been well known for quite some time that the accuracy of physical representation of the actual turbulence fields depends on the order of closure of the transport equations describing turbulence. Thus the model succeeding the two-equation model is that of second-order closure, or the

Reynolds-stress closure. This type of higher-order modeling has been used quite successfully by Launder, et. al., [19], [20] for channel and boundary layer type flows. Though there is no conceptual difficulty in using this model along with the mean Navier-Stokes equations, the discouragement on its use stems from the excessive computational requirements in the form of solving three or six additional partial differential equations for two- or three-dimensional problems respectively. A class of closure which can reasonably be thought of as equivalent to the second-order closure and called the "algebraic stress closure" has been developed by Launder, et. al., [21] and Warsi, et. al., [22] and is described below.

The basic equation for the present consideration is now Eq. (24). Following the analysis in Warsi [22], the Reynolds stress term $\bar{\tau}_{ij}$ can be approximated, on using Eq. (24), as

$$\bar{\tau}_{ij} = \frac{2}{3}\bar{e}\,\delta_{ij} + \frac{\gamma_o \bar{e}}{\bar{P} + d_1\bar{\varepsilon}}\left(\bar{P}_{ij} - \frac{2}{3}\bar{P}\,\delta_{ij}\right) \tag{51}$$

where all quantities have been defined earlier, and $\gamma_o = 0.6$, $d_1 = 0.8$. The accuracy of representation (51) depends on the plausible assumption that the substantive rate of change of $\bar{\tau}_{ij}/\bar{e}$ in following the mean motion is small in comparison with the other terms, viz.,

$$\bar{e}\,\frac{d}{dt}\left(\frac{\bar{\tau}_{ij}}{\bar{e}}\right) << \frac{\bar{\tau}_{ij}}{\bar{e}}\,\frac{d\bar{e}}{dt} \tag{52}$$

Equations (51) form a system of non-linear algebraic equations for the determination of various Reynolds stresses to be used in a two-equation model. However, assuming the Reynolds stresses in $\bar{P}$ to be available from the previous iteration, the equations can be solved as linear simultaneous algebraic equations for $\bar{\tau}_{ij}$. The results presented

below are for the case of two-dimensional mean flow in the vorticity-stream function formulation. The closure for the unknown terms for the two-equation model is due to Launder [20]. All quantities appearing below are non-dimensional.

Defining the quantities

$$\left.\begin{aligned} S_{11} &= \psi_{xx} \ , \ S_{12} = \psi_{xy} \ , \ S_{22} = \psi_{yy} \\ T_1 &= \frac{\partial^2 \tau_{12}}{\partial x^2} \ , \ T_2 = \frac{\partial^2 \tau_{12}}{\partial y^2} \\ T_3 &= \frac{\partial^2 \tau_{11}}{\partial x \partial y} \ , \ T_4 = \frac{\partial^2 \tau_{22}}{\partial y^2} \\ M_1 &= \frac{C_s E}{\varepsilon} (\tau_{11} E_x + \tau_{12} E_y) \\ M_2 &= \frac{C_s E}{\varepsilon} (\tau_{12} E_x + \tau_{22} E_y) \\ N_1 &= \frac{C_o E}{\varepsilon} (\tau_{11} \varepsilon_x + \tau_{12} \varepsilon_y) \\ N_2 &= \frac{C_o E}{\varepsilon} (\tau_{12} \varepsilon_x + \tau_{22} \varepsilon_y) \end{aligned}\right\} \qquad (53)$$

where τ_{ij} is the non-dimensional Reynolds stress, and $C_o = 0.15$, $C_s = 0.22$. Thus

$$P = (\tau_{22} - \tau_{11}) \, S_{12} + (S_{11} - S_{22}) \tau_{12}$$

$$Z_o = \frac{\gamma_o E}{P + d_1 \varepsilon}$$

$$Z = Z_o{}^2 (4\omega S_{22} + S_{12}{}^2 + S_{22}{}^2 - 2\omega^2) - 3$$

$$\tau_{11} = \frac{-2E}{Z} (1 - 2 Z_o S_{12} - 2 Z_o{}^2 \omega S_{22})$$

$$\tau_{12} = \frac{2E}{Z} \{Z_o (S_{22} - S_{11}) - 2 Z_o{}^2 \omega S_{12}\} \qquad (54)$$

$$\tau_{22} = \frac{-2E}{Z} (1 + 2 Z_o S_{12} - 2 Z_o{}^2 \omega S_{11})$$

The complete set of equations is

$$D^2\psi + \tau\psi_\xi + \sigma\psi_\eta = -g\omega \qquad (55)$$

$$F_t + \frac{1}{g^{1/2}} (F_\xi \psi_\eta - F_\eta \psi_\xi) = \frac{1}{gR_o} (D^2 F + \tau F_\xi + \sigma F_\eta) + T_F \qquad (56)$$

where F is a surrogate variable. The forms of T_F for different equations are as follows:

For F = ω:

$$T_\omega = T_2 + T_3 - T_1 - T_4$$

For F = E:

$$T_E = F + \frac{1}{g^{1/2}} \left(y_\eta \frac{\partial M_1}{\partial \xi} - y_\xi \frac{\partial M_1}{\partial \eta} + x_\xi \frac{\partial M_2}{\partial \eta} - x_\eta \frac{\partial M_2}{\partial \xi}\right) \qquad (57)$$

For F = ε:

$$T_\varepsilon = \frac{C_1' \varepsilon P}{E} - \frac{C_2 \varepsilon^2}{E}$$

$$+ \frac{1}{g^{1/2}} \left(y_\eta \frac{\partial N_1}{\partial \xi} - y_\xi \frac{\partial N_1}{\partial \eta} + x_\xi \frac{\partial N_2}{\partial \eta} - x_\eta \frac{\partial N_2}{\partial \xi}\right)$$

where

$$C_1' = 1.44 \ , \ C_2 = 1.9$$

3.1.9 Collection of Various Formulae and Approximations

All the formulae listed below are non-dimensional.

(a) Friction Velocity:

$$U_*^2 = \frac{|\omega_w|}{R_o} \tag{58a}$$

(b) Local Skin Friction Coefficient:

$$C_f = \frac{2|\omega_w|}{R_o U_p^2} \tag{58b}$$

where

$$U_p = \text{MAX}\ (U_s)$$

$$U_s = \sqrt{\frac{g_{11}}{g}}\,\psi_\eta - \frac{g_{12}}{\sqrt{g g_{11}}}\,\psi_\xi$$

(c) Reynolds Shear Stress:

$$\frac{\overline{u_1' u_2'}}{u_\infty^2} = -T(\psi_{yy} - \psi_{xx}) \tag{58c}$$

(d) Pressure Coefficient:

The wall pressure $\bar{p}_w$ non-dimensionalized by ρu_∞^2 is given by

$$p_w(\xi) = p_w(\xi_{ref}) + \frac{1}{R_o}\int_{\xi_{ref}}^{\xi} \frac{1}{g^{1/2}}\,(g_{12}\omega_\xi - g_{11}\omega_\eta)\,d\xi$$

Now, the pressure coefficient is defined as

$$C_p = \frac{\bar{p}_w(\ ) - \bar{p}}{\frac{1}{2}\rho u_\infty^2}$$

Thus

$$C_p = 2[p_w(\xi) - p_\infty]\ . \tag{58d}$$

(e) Transition Factor:

In this paper the Cebeci-Smith transition factor γ_{tr} [23] was used to multiply the eddy viscosity to account for the transition region. In non-dimensional variables, γ_{tr} is given by

$$\gamma_{tr} = 1 - \text{Exp}\left[\frac{-R_o^{.66} U_p^{-1.66} S_{tr}^{-1.34}(S - S_{tr})}{1200} \int_{s_{tr}}^{s} \frac{ds}{U_p}\right] \qquad (58e)$$

where S_{tr} denotes the surface distance of the location of transition.

(f) Boundary Conditions for E and χ Very Near to the Wall:

In the immediate vicinity of a wall the low Reynolds number effects on turbulence quantities are quite significant. Though the generated coordinate mesh is very fine near the wall region for all cases considered here, the viscous resolution still demands much finer meshes. To circumvent this difficulty we have used approximate analytic expressions for E and χ for the first mesh point off the wall. The form of E used here is based on the analysis of Launder, et. al., [21] for the wall-viscous effects. In non-dimensional variables the expression for E is

$$E \simeq .0275|\omega_w|^2 N^2 \text{ , as } N \to o \text{ .} \qquad (58f)$$

To obtain the form of χ as $N \to o$, we use Townsend's expression for the dissipation function for equilibrium boundary layers [24], which, for near wall regions is

$$\chi = \frac{0.4E^{3/2}}{N} \text{ .}$$

Using (58f), we get

$$\chi = .001824|\omega_w|^3 N^2 \text{ , as } N \to o \text{ .} \qquad (58g)$$

Note that in principle $E \to o$ at the wall in such a way that $\chi \to \infty$. However, as observed by Daly and Harlow [25], the tendency of χ to become infinite

occurs only in the sublayer; outside the variation of χ can be such as to give the appearance of approaching zero at the wall.

4. Numerical Solution of the Transport Equation

This section deals with the computational aspects of the equations governing the mean turbulent flow fields. Besides the method of numerical solution, we shall also discuss the method of generation of initial data for the solution of the energy and the dissipation equations, and the wall boundary condition for the vorticity equation.

4.1 Method of Solution:

All the partial differential equations are first discretized by using a first order backward difference for the time derivative and the second order central differences for the ξ and η derivatives. The resulting system of difference equations is then solved by iteration using the method of point-successive overrelaxation (SOR). Using the model equation (12), the SOR difference approximation amounts to having the implicit expression

$$\lambda_{i,j}^{(p+1)} = \lambda_{i,j}^{(p)} + WR_{i,j} \tag{59}$$

where p is an iteration counter, (i,j) denote the spatial position, $R_{i,j}$ is the residual term containing the previous time solution and the previous iterative solutions at the neighboring points, and W is the acceleration parameter. For details of difference approximation of the two-equation model refer to [18]. Convergence of the iteration is obtained by satisfying the inequality

$$|\lambda_{i,j}^{(p+1)} - \lambda_{i,j}^{(p)}|/|\lambda_{i,j}^{(p+1)}| < \varepsilon_o \tag{60}$$

for all points of the field.

In the solution of the vorticity equation, viz., equation (30), it was found that the upwind differencing of the term $\psi_\eta \omega_\xi$ enhances the stability of the difference approximation [26]. Thus, for only the vorticity equation

the upwind differencing for the term $\psi_\eta \omega_\xi$ has been used, which is

$$\psi_\eta \omega_\xi \simeq \begin{cases} (\psi_\eta)_{i,j} \, (\omega_{i,j} - \omega_{i-1,j}) \, , \; \psi_\eta \geq o \\ (\psi_\eta)_{i,j} \, (\omega_{i+1,j} - \omega_{i,j}) \, , \; \psi_\eta < o \end{cases} \tag{61}$$

The method of solution for turbulence problems can now be summarized as follows. Having developed the numerical coordinates for a given body, all the metric coefficients are generated numerically. First the equations for the laminar flow, in the present case the vorticity and stream function equations, are solved starting from time t = o. Usually the laminar solution is allowed to develop to a quasi-steady state form and then turbulence equations are introduced. In no case, except in [27], the turbulence was introduced at t = o. In the process of obtaining the laminar solution, the initial data for the E and χ equations (described in Sect. 4.2 below) are also developed simultaneously. Having available the velocity field and the initial data for E and χ, it becomes an easy task to switch on to the simultaneous solution of all the equations. The choice of the turbulence model, location of the beginning of transition, and the amount of free-stream turbulence are the inputs for a problem which can all be handled easily by the computer program used in the present research. The computer program also calculates the necessary boundary layer parameters, e.g., displacement and the momemtum thickness, external velocity, etc.

4.2 Initial Data for the E-and χ Equations:

The approximate generation of initial data depends on some well known forms for the eddy viscosity ν_T and the dissipation function $\bar{\varepsilon}$. From (32a), we have

$$\nu_T = \ell^2 (\bar{\Omega})^{1/2}$$

$$= \frac{(\alpha_o \bar{e})^2}{\bar{\varepsilon}}$$

$$\bar{\varepsilon} = \frac{(\alpha_o \bar{e})^{3/2}}{\ell} \tag{62}$$

where $\alpha_o = 0.3$. Using the non-dimensionalization introduced in Sect. 3, we obtain from Eqs. (62)

$$E = \frac{1}{\alpha_o} \Lambda^2 Q$$

$$\chi = \Lambda^2 Q^{3/2} \tag{63}$$

As noted in Sect. 4.1, Eqs. (63) are used while solving the laminar equations. The generated values of E and χ are then used as the initial data for the solution of the turbulence model equations.

4.3 Wall-Vorticity:

The wall-vorticity is obtained by using a combination of the Israeli method [28] and a modification proposed in [18]. The value of wall-vorticity is assumed to be correct when it yields a vanishing tangential velocity at the wall. Denoting the index i for the position along a wall and p the iteration counter, the iterative expression for the wall-vorticity is given by

$$\omega_i^{(p+1)} = \omega_i^{(p)} - \frac{\omega_i^{(p)} - \omega_i^{(p-1)}}{v_{(t)i}^{(p)} - v_{(t)i}^{(P-1)}} v_{(t)i}^{(p)} \tag{64}$$

where $v_{(t)}$ is the tangential velocity component at the wall.

5. Discussion of Results

The mathematical models of various orders developed in Section 3 have been used to compute the two-dimensional incompressible mean turbulent flows past arbitrary finite-bodies. A computer program based on the finite difference method as discussed in Section 4 has been used to obtain the flow fields for various body shapes. The difference from one body shape to another is only in the input of the metric data and the coordinates for each body which are obtained by separate programs, e.g., [12]. The following three shapes have been extensively studied and their results are discussed below.

(a) Elliptical cylinder at zero incidence.
(b) NACA 66_3-018 airfoil at zero incidence.
(c) Circular cylinder.

In all the above cases, the free stream is normal to the axis of the cylinders.

5.1 Elliptical Cylinder

The calculations for this case are based on the input data from Schubauer's [28] experimental set up. The elliptical section is of minor axis 10.11 cm, major axis 29.92 cm and is exposed to a uniform stream of Reynolds number R_o of 1.59×10^5 based on the minor axis. The free stream turbulence level E_∞ is 0.1084×10^{-3}.

The characteristic length L for this problem is the minor axis which has been used to non-dimensionalize all lengths. A highly contracted coordinate system is used near the wall region to resolve the viscous effects in the boundary layer. The coordinate plot is shown in Figure 2.

The transition model, Eq. (58e), was introduced in the region $1.5 \leq \frac{s}{L} \leq 1.8$, where s is the arc length along the surface measured from the forward stagnation point. From $\frac{s}{L} = 1.8$ to $\frac{s}{L} = 3.3048$ the full

turbulence model has been used. The laminar solution was continued from $t_1 = o$ to a time $\frac{2L}{U_\infty}$ and then the zero-equation model was used with the transition effects included to a time $\frac{3L}{U_\infty}$. Based on this solution, the one-equation model was used to conclude the solution process. As is seen from the velocity vector plots in Figure 3, the separation occurs in the far downstream region very near to the trailing edge. It is because of this reason that we have compared the computed pressure coefficient with Schubauer's [8] curve B, and the comparison seems satisfactory, (Fig. 4).

In Figure 5 the coefficient of skin friction c_f is compared with the Schubauer's data as reproduced by Cebeci and Smith [23]. The skin friction coefficient in the turbulent part of the flow is computed by the formula $U_1^2 c_f = 0.6\, E_s$, where E_s is the turbulence energy at the edge of the sublayer. Figure 6 shows the turbulence energy contours around the ellipse.

5.2 NACA66$_3$-018 Airfoil

The results presented for this case are for zero incidence at a chord Reynolds number R_o of 1.2×10^6. In this case too, there is a strong contraction of coordinates near the surface so as to have at least 20 η-lines in the boundary layer. Figure 7 shows the plot of the coordinate lines around the airfoil. As seen from Fig. 7, the coordinates are generally non-orthogonal.

Experimental data on NACA66$_3$-018 section is available in the papers by Bursnall and Loftin [29] and Gault [30]. Numerical computation on this section has been performed by Briley and McDonald [26] particularly with the idea of performing the Navier-Stokes analysis on the separation bubbles. In Ref. [26], a laminar boundary layer solution is patched with the Navier-Stokes separation bubble analysis which is finally patched with the turbulent boundary layer solution downstream of the bubble region.

In the present computations the Navier-Stokes solution was generated for the whole surface both for the laminar and turbulence cases without any indication of a separation bubble at $R_o = 1.2 \times 10^6$. The velocity vector plot in Figure 8 shows no indication of a flow reversal or recirculation region at the expected position. The transition model was introduced at the expected position of the transitional bubble which is nearly $\frac{s}{L} \simeq 0.72$, where L is the chord length.

The computed pressure coefficient for this case is shown in Figure 9. Figures 10 and 11 show the turbulence energy contours and the streamlines respectively. Only zero and one-equation models were used in this study with the free stream turbulence $E_\infty = .3375 \times 10^{-5}$.

5.3 Circular Cylinder

The turbulent flow past a circular cylinder has been considered by the authors in [27]. Details of computational analysis are available in [18]. In the present case the two-equations model as developed by Saffman and Wilcox [17] has been used. Results of this computation are shown in Figures 12-16 for a Reynolds number $R_o = 1.4 \times 10^6$ based on the radius of the cylinder.

6. Conclusions

Solutions of the averaged Navier-Stokes equations along with the equations of turbulence quantities have been obtained for various body shapes in non-orthogonal curvilinear body-fitted coordinate systems. In principle, the developed computer program is capable of predicting the averaged flow and turbulence fields around any fintie two-dimensional body, using either the zero, one, or two-equations turbulent closure model. In addition, an algebraic stress closure model has also been developed which can be used with any two-equation model for predicting the flow fields having large separation and recirculating regions.

Appendix A

Let x_i be the Cartesian coordinates and ξ^i the general curvilinear coordinates. Then the metric coefficients are

$$g_{ij} = \frac{\partial x_k}{\partial \xi^i} \frac{\partial x_k}{\partial \xi^j} \tag{A-1}$$

$$g^{ij} = \frac{\partial \xi^i}{\partial x_k} \frac{\partial \xi^j}{\partial x_k} \tag{A-2}$$

$$g^{ik} g_{jk} = \delta^i_j \tag{A-3}$$

$$g = \det (g_{ij}) \tag{A-4}$$

$$J = g^{1/2} = \frac{\partial (x_1, x_2, x_3)}{\partial (\xi^1, \xi^2, \xi^3)} \tag{A-5}$$

Using the summation convention on repeated indices, the Christoffel symbols of the second kind are given by

$$\Gamma^i_{jk} = \frac{1}{2} g^{i\ell} \left(\frac{\partial g_{\ell j}}{\partial \xi^k} + \frac{\partial g_{\ell k}}{\partial \xi^j} - \frac{\partial g_{jk}}{\partial \xi^\ell} \right) \tag{A-6}$$

In particular

$$\Gamma^k_{kr} = \frac{1}{2g} \frac{\partial g}{\partial \xi^r} \tag{A-7}$$

References

1. Reynolds, W. C., "Computation of Turbulent Flows," Annual Review of Fluid Mechanics, 8, 183 (1976).

2. Thompson, J. F., Thames, F. C., and Mastin, C. W., "Automatic Numerical Generation of Body-Fitted Curvilinear Coordinate System for Field Containing any Number of Arbitrary Two-Dimensional Bodies," Journal of Computational Physics, 15, 299 (1974).

3. Warsi, Z. U. A., Devarayalu, K., and Thompson, J. F., Numerical Solution of the Navier-Stokes Equations for Arbitrary Blunt Bodies in Supersonic Flows," Numerical Heat Transfer, 1, 499 (1978).

4. Shamroth, S. J., and Gibeling, H. J., "The Prediction of the Turbulent Flow Field about an Isolated Airfoil," AIAA Paper No. 79-1543, (1979).

5. Eiseman, P. R., "A Coordinate System for a Viscous Transonic Cascade Analysis," Journal of Computational Physics, 26, 307 (1978).

6. Davis, R. T., "Numerical Methods for Coordinate Generation Based on Schwarz-Christoffel Transformations," AIAA Paper, No. 79-1463, (1979).

7. Roache, P. J., "Computational Fluid Dynamics," Hermosa Publishers, Albuquerque, N.M., (1976).

8. Schubauer, G. B., "Air Flow in the Boundary Layer of an Elliptic Cylinder," NACA Report No. 652, (1939).

9. Glushko, G. S., "Turbulent Boundary Layer on a Flat Plate in an Incompressible Fluid," Bull. Acad. Sci. USSR, Mech. Ser., No. 4, 13 (1965).

10. Saffman, P. G., "Model Equations for Turbulent Shear Flow," Studies in Appl. Math., 53, 17 (1974).

11. Thompson, J. F., Thames, F. C., and Mastin, C. W., "TOMCAT-A Code for Numerical Generation of Boundary-Fitted Curvilinear Coordinate Systems on Fields Containing any Number of Arbitrary Two-Dimensional Bodies," Journal of Computational Physics, 24, 274 (1977).

12. Thames, F. C., "Numerical Solution of the Incompressible Navier-Stokes Equations about Arbitrary Two-Dimensional Bodies," Ph.D. Dissertation, Mississippi State University (1975).

13. Warsi, Z. U. A., and Thompson, J. F., "Machine Solutions of Partial Differential Equations in the Numerically Generated Coordinate Systems," Report MSSU-EIRS-ASE-77-1, Engineering and Industrial Research Station, Mississippi State University, (1976).

14. Coakley, T. J., and Bergmann, M. Y., "Effects of Turbulence Model Selection on the Prediction of Complex Aerodynamic Flows," AIAA Paper No. 79-0070, (1979).

15. Bradshaw, P., "The Turbulence Structure of Equilibrium Boundary Layers," Journal of Fluid Mechanics, 29, 625 (1967).

16. Beckwith, I. E., and Bushnell, D. M., "Detailed Description and Results of a Method for Computing Mean and Fluctuating Quantities in Turbulent Boundary Layers," NASA TND-4815, (1968).

17. Wilcox, D. C., and Traci, R. M., "A Complete Model of Turbulence," AIAA Paper No. 76-351, (1976).

18. Amlicke, B. B., "Numerical Solution of the Two-Dimensional Non-Steady Mean Navier-Stokes Equations for Incompressible Flows Past Arbitrary Shaped Bodies," Ph.D. Dissertation, Mississippi State University, December (1978).

19. Launder, B. E., Reece, G. J., and Rodi, W., "Progress in the Development of a Reynolds-Stress Turbulence Closure," Journal of Fluid Mechanics, 68, 537 (1975).

20. Hanjalic, H., and Launder, B. E., "Contribution Towards a Reynolds-Stress Closure for Low-Reynolds-Number Turbulence," Journal of Fluid Mechanics, 74, 593 (1976).

21. Sha, W. T., and Launder, B. E., "A General Model for Turbulent Momentum and Heat Transport in Liquid Metals," Argonne National Laboratory, ANL-77-78, November, (1977).

22. Warsi, Z. U. A., and Amlicke, B. B., "Improved Algebraic Relation for the Calculation of Reynolds Stresses," AIAA Journal, 14, 1779 (1976).

23. Cebeci, T., and Smith, A. M. O., "Analysis of Turbulent Boundary Layers," Academic Press (1974).

24. Townsend, A. A., "The Structure of Turbulent Shear Flow," Cambridge University Press (1976).

25. Daly, B. J., and Harlow, F. H., "Transport Equations in Turbulence," Physics of Fluids, 13, 2634 (1970).

26. Briley, W. R., and McDonald, H., "Numerical Prediction of Incompressible Separation Bubbles," Journal of Fluid Mechanics, 69, 631 (1975).

27. Thompson, J. F., Warsi, Z. U. A., and Amlicke, B. B., "Numerical Solutions for Laminar and Turbulent Viscous Flow over Single and Multi-Element Airfoils Using Body-Fitted Coordinate Systems," Advances in Engineering Science, NASA CP-2001 (1976).

28. Israeli, M., "A Fast Implicit Method for Time Dependent Viscous Flows," Studies in Applied Math., 49, 327 (1970).

29. Bursnall, W. J., and Loftin, L. K., "Experimental Investigation of Localized Regions of Laminar-Boundary-Layer Separation," NACA TN 2338 (1951).

30. Gault, D. E., "An Experimental Investigation of Regions of Separated Laminar Flow," NACA TN 3505 (1955).

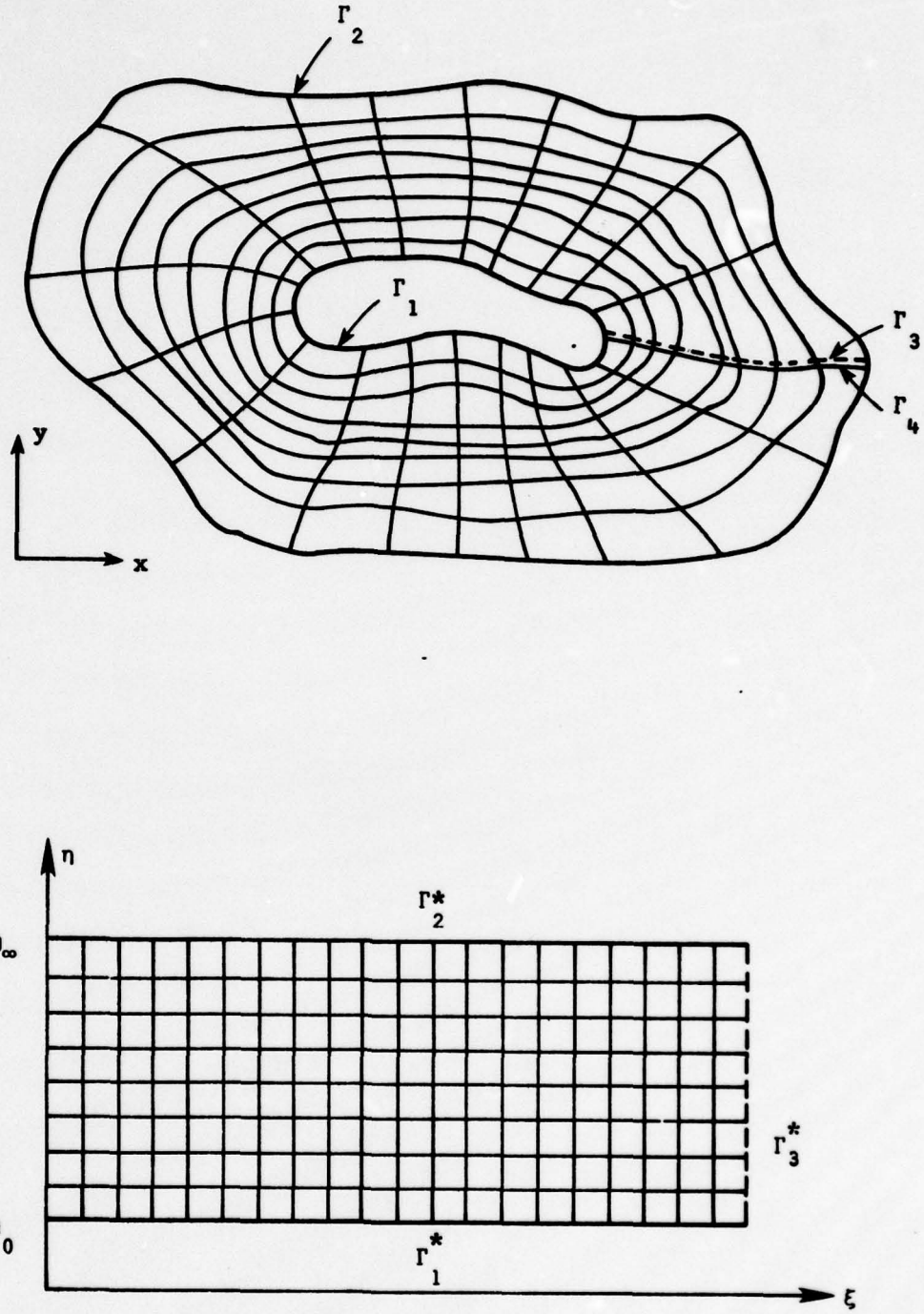

Figure 1. Physical and Transformed Planes.

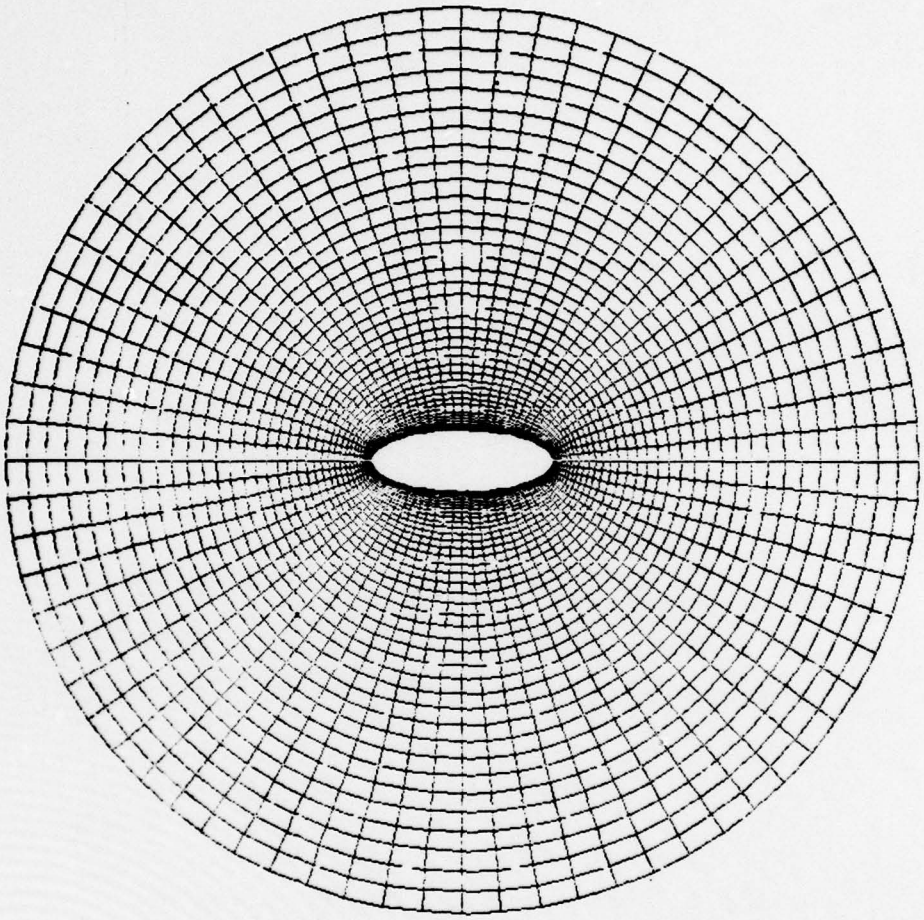

Figure 2. Generated Coordinate Plot for the Schubauer's Ellipse.

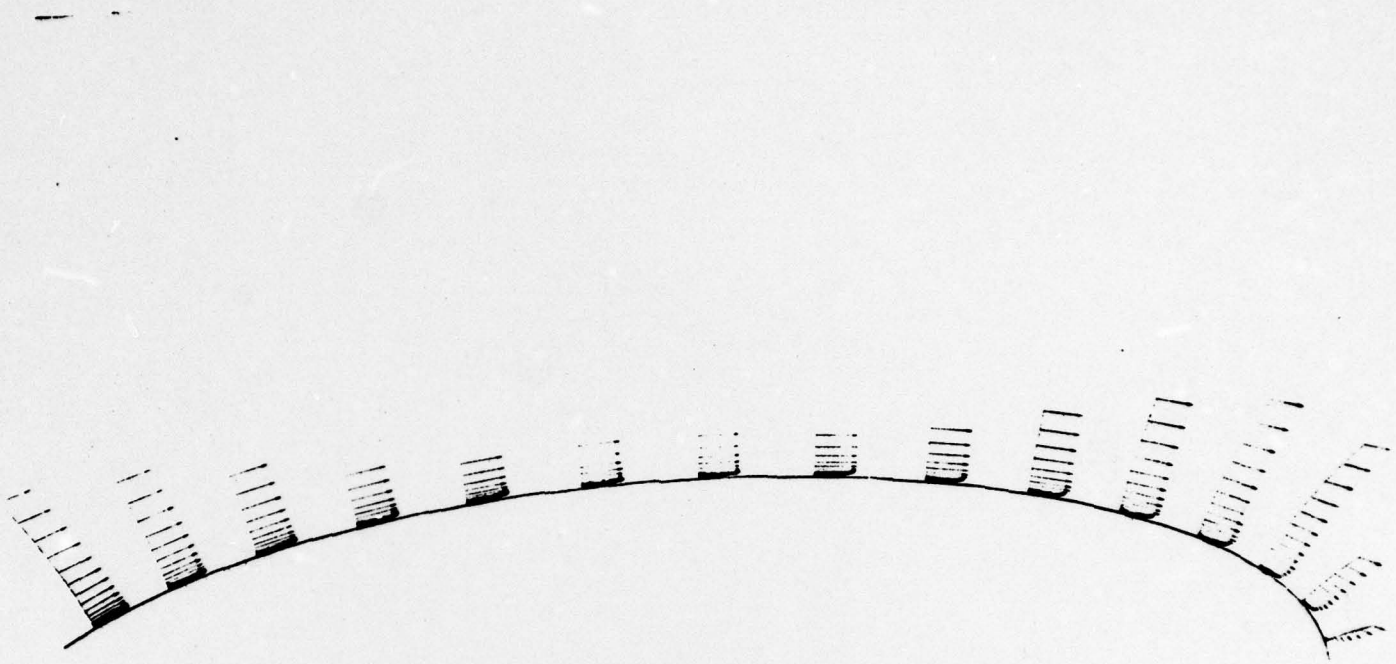

Figure 3. Velocity Vector Plots for Various Positions on the Ellipse Versus η.

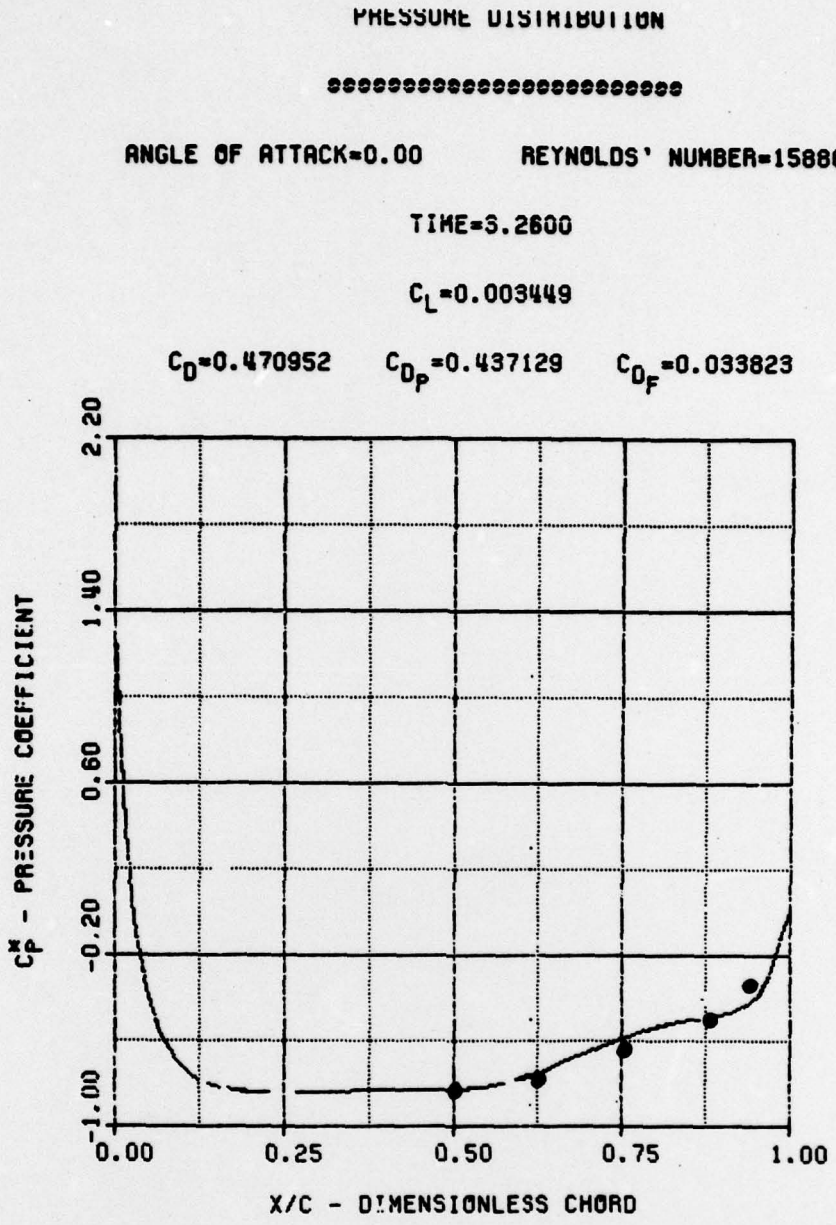

Figure 4. Pressure Coefficient, C_p. ● Data from Ref. [8].

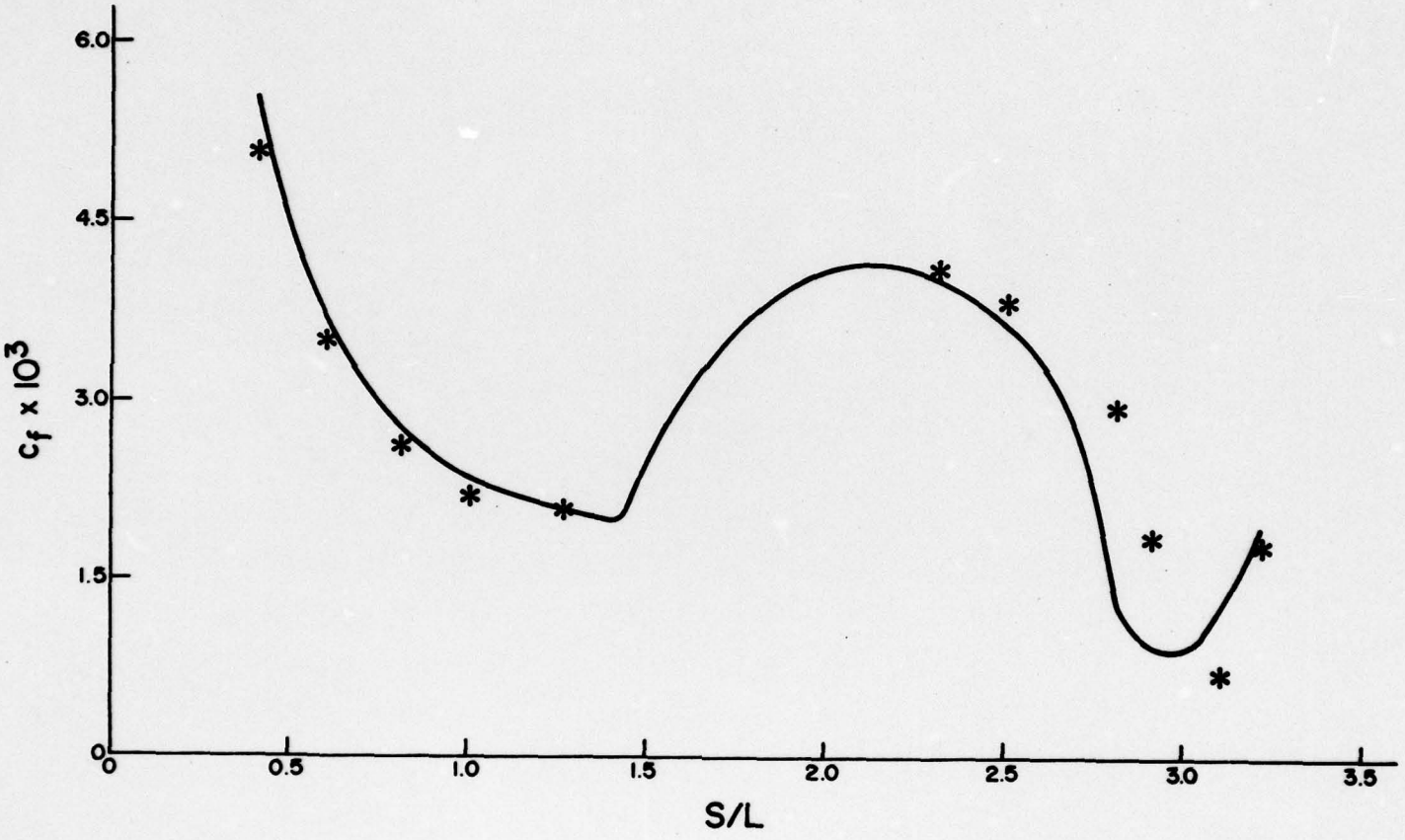

Figure 5. Coefficient of Skin-Friction C_f from Ref. 23, * - Data from Present Calculations.

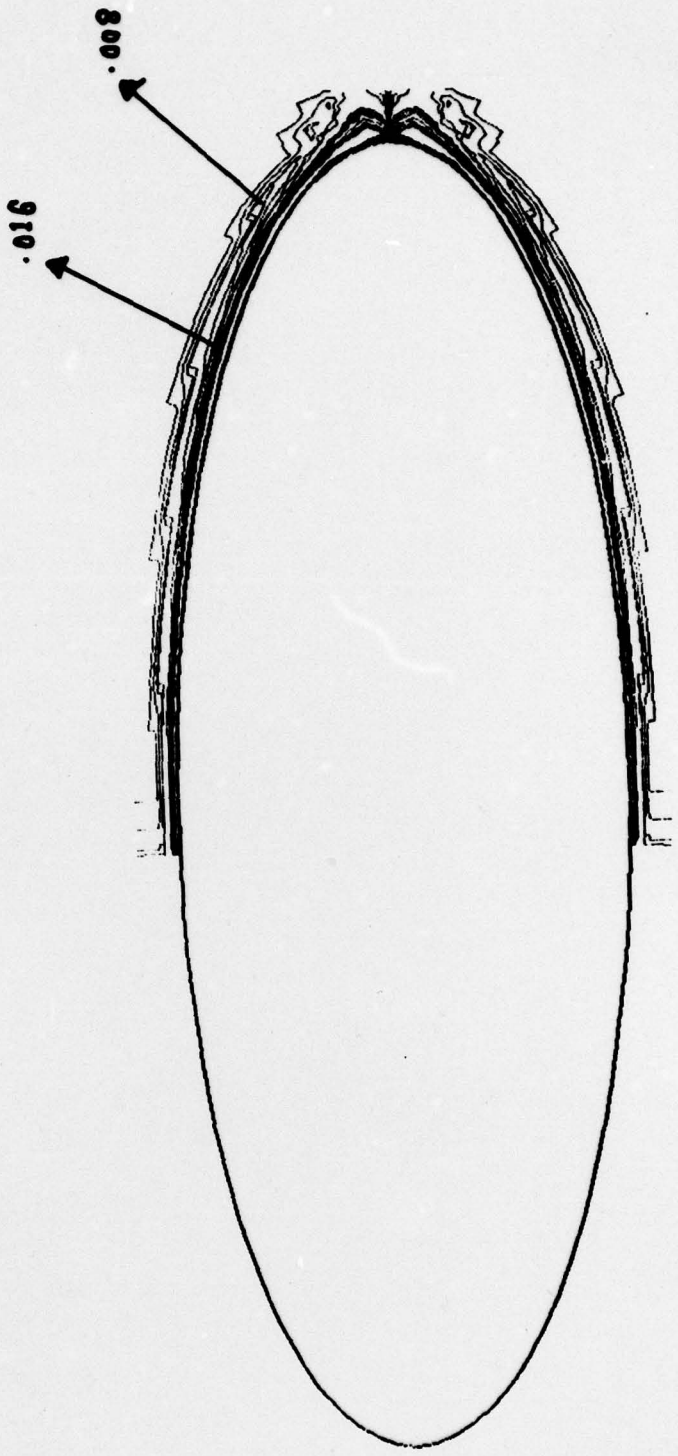

Figure 6. Turbulent Energy Contours.

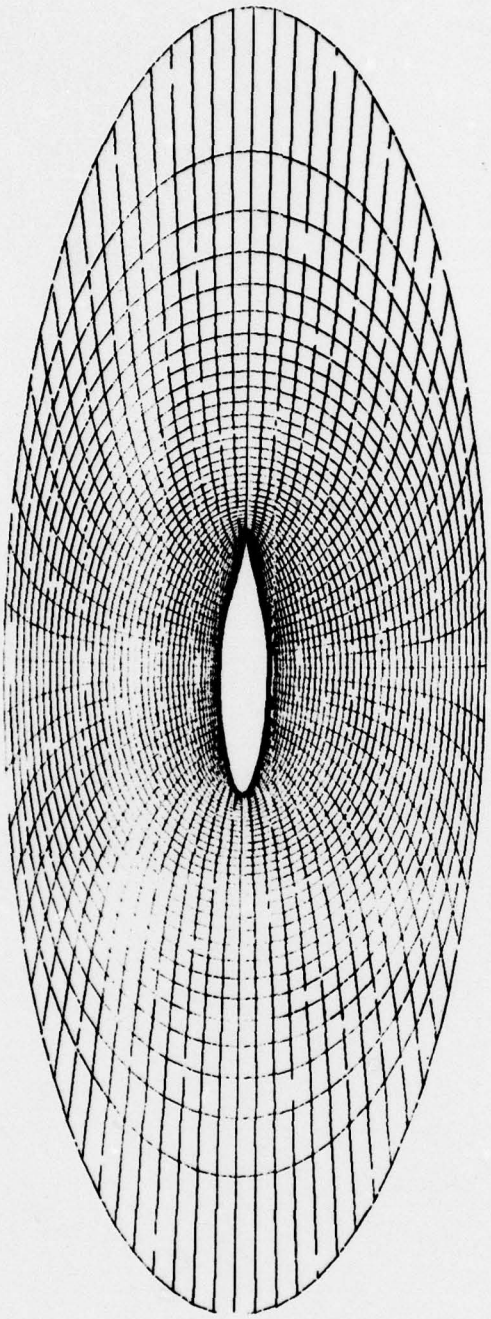

Figure 7. Generated Coordinate Plot for the NACA66_3-018 Airfoil.

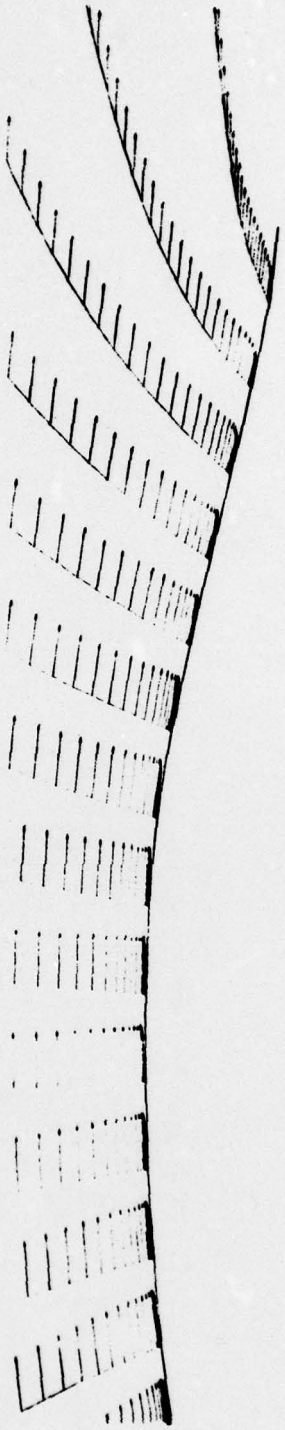

Figure 8. Velocity Vector Plots for Various Positions on the Airfoil Versus η.

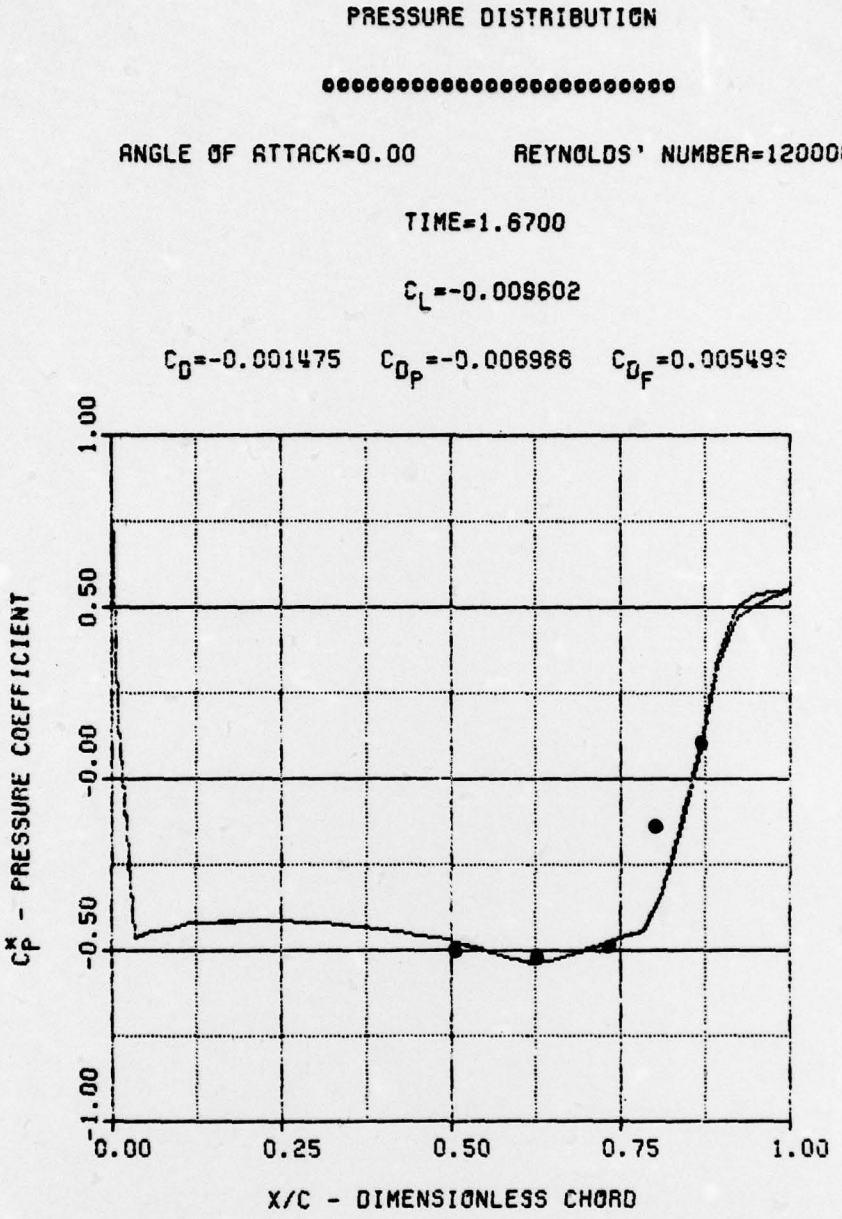

Figure 9. Pressure Coefficinet C_p. ● Data from Ref. [30].

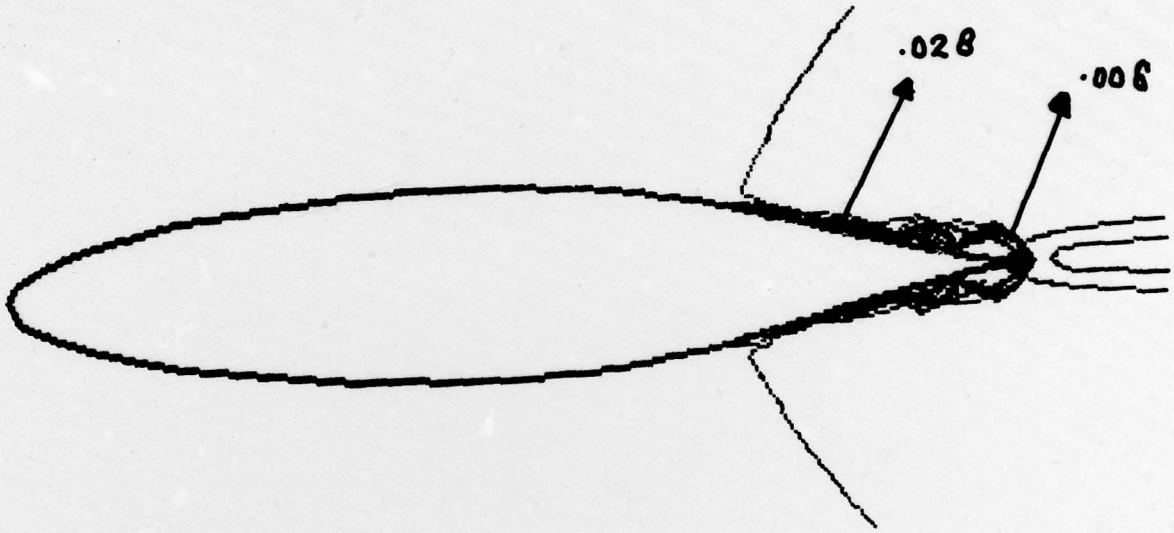

Figure 10. Turbulent Energy Contours.

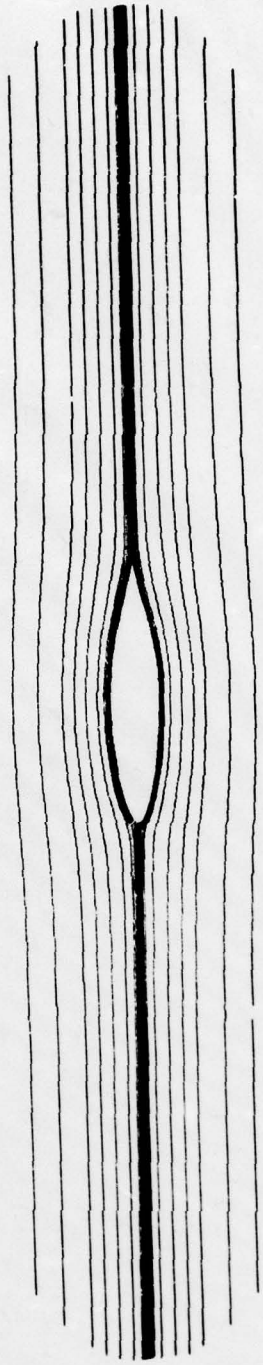

Figure 11. Stream Function Plot on the Airfoil.

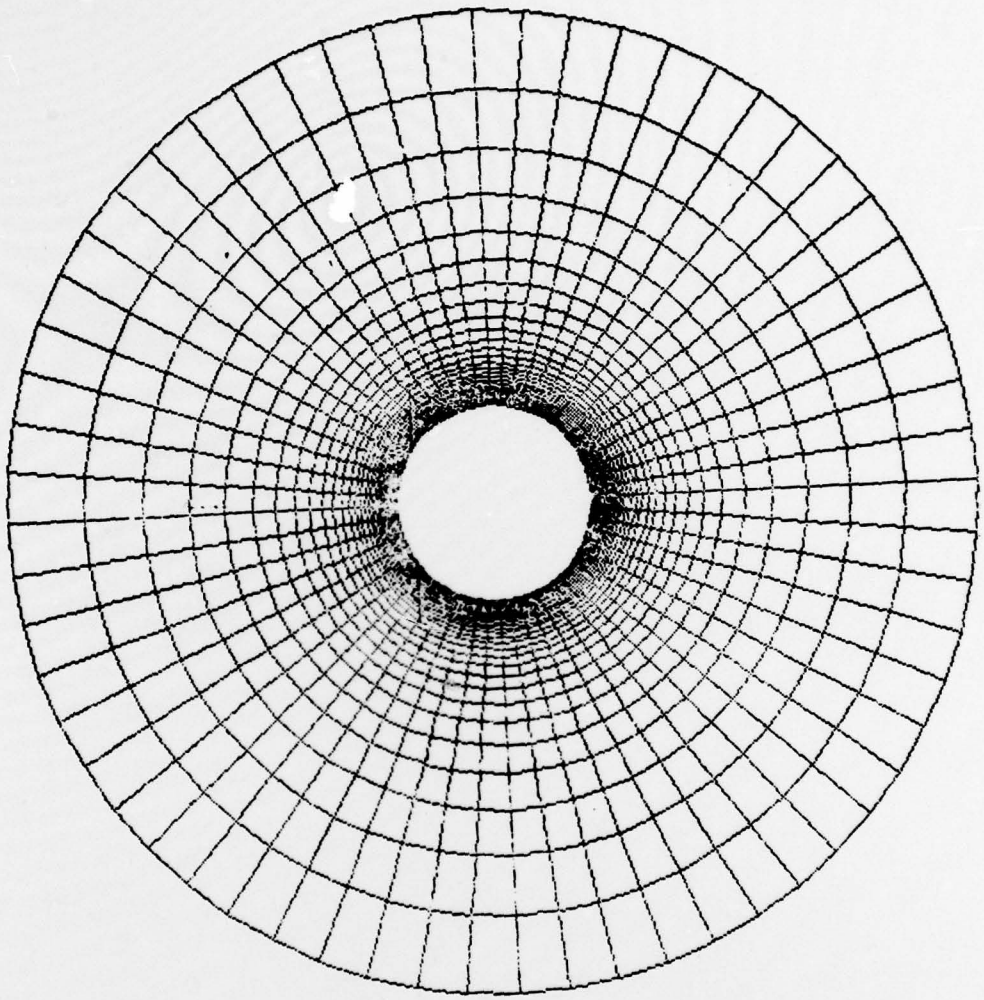

Figure 12. Generated Coordinates for the Circle.

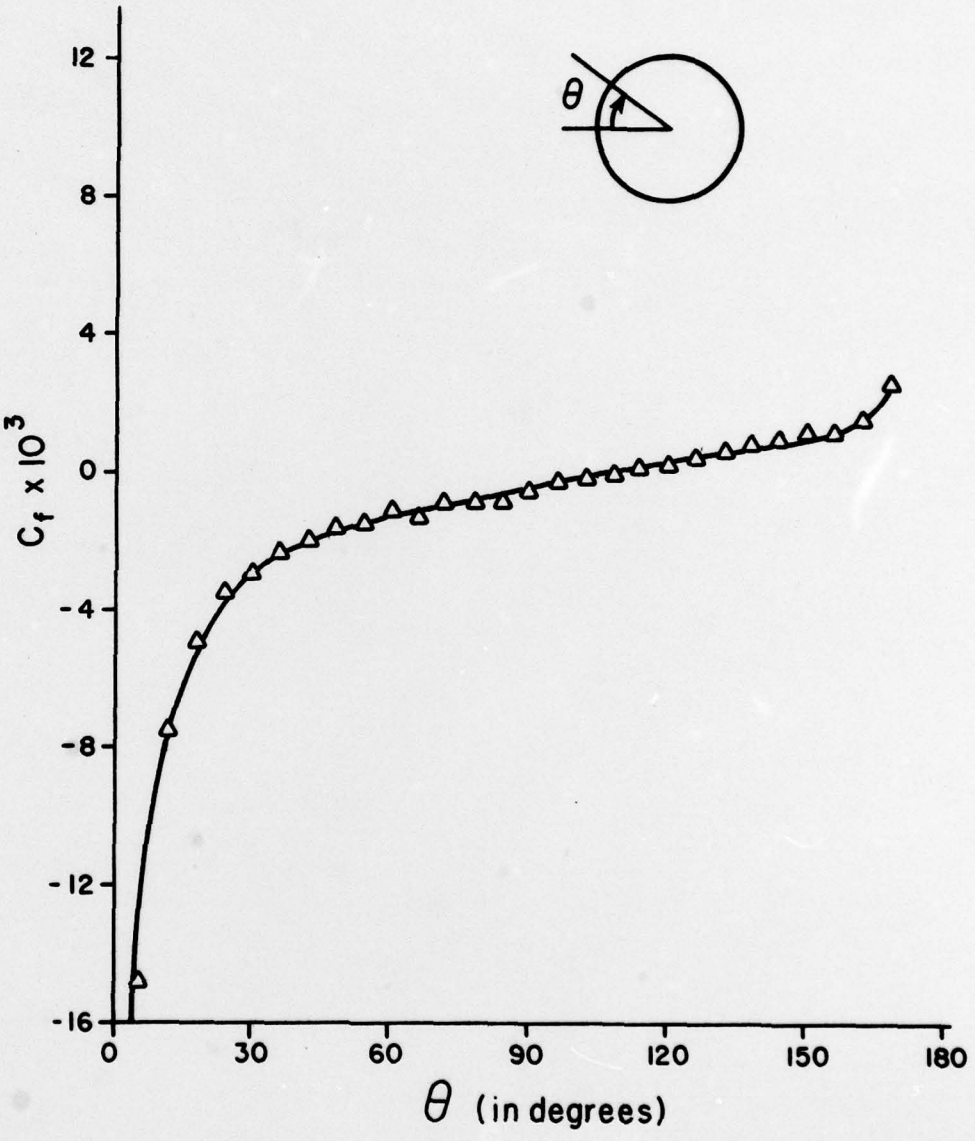

Figure 13. Local Skin Friction (c_f) where $c_f = \tau_w / 1/2\ \rho u_p^2$.

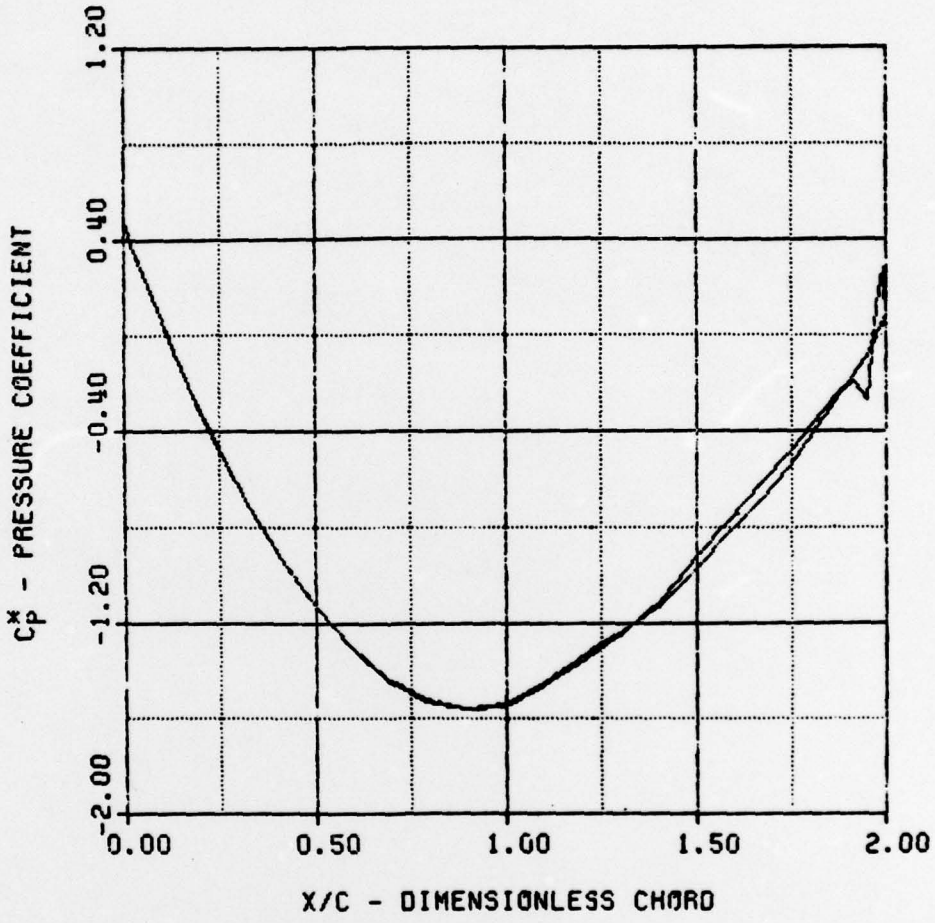

Figure 14. Coefficient of Pressure (C_p^*) Referenced to a Rear Stagnation Pressure of 1.0. C_p is $p - p_{T.E.}$. The Total Drag Coefficient C_D is .293 where $C_D = D/\rho\ v_\infty^2\ r_e$.

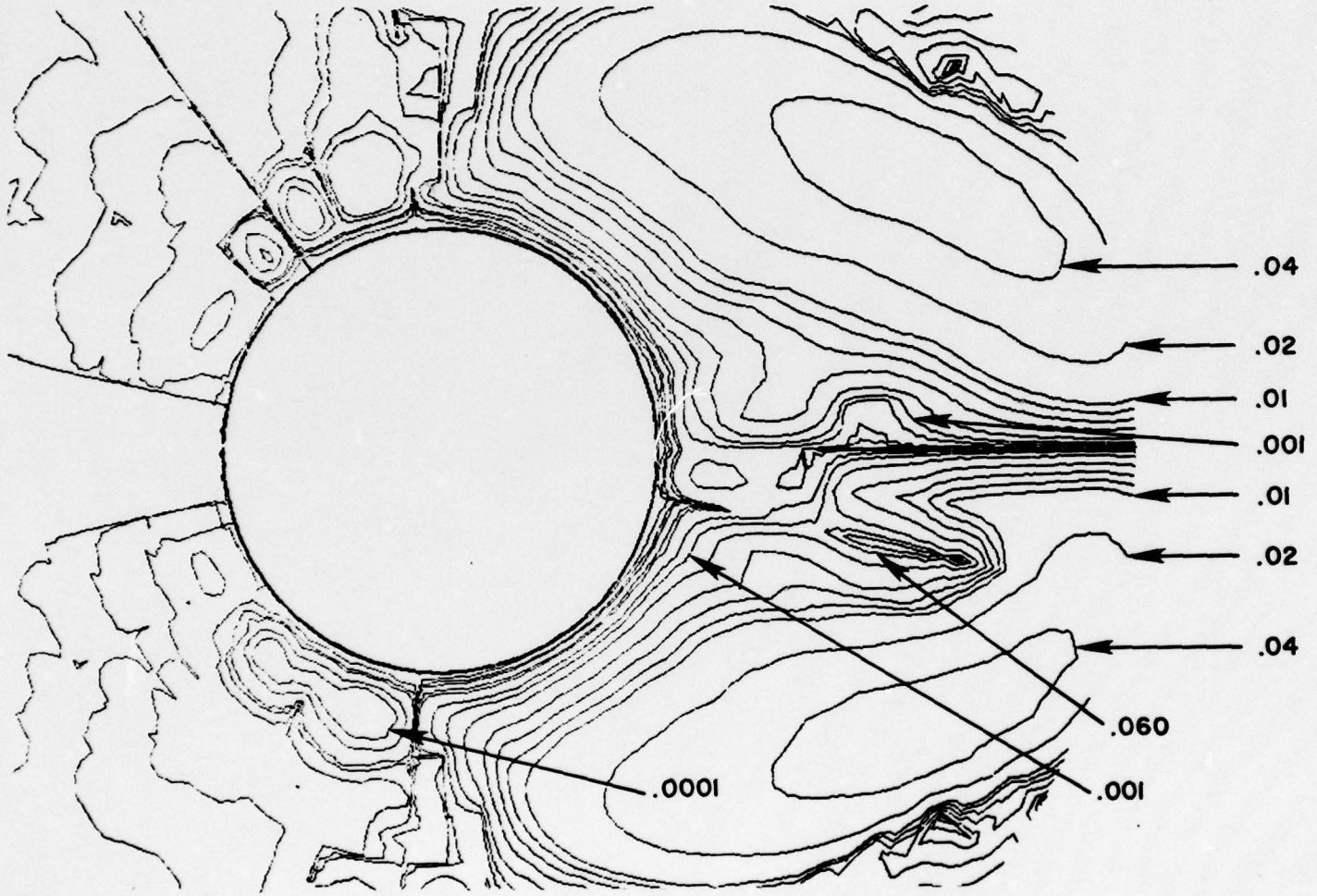

Figure 15. Mean Turbulent Energy Contours at Time 3.72.

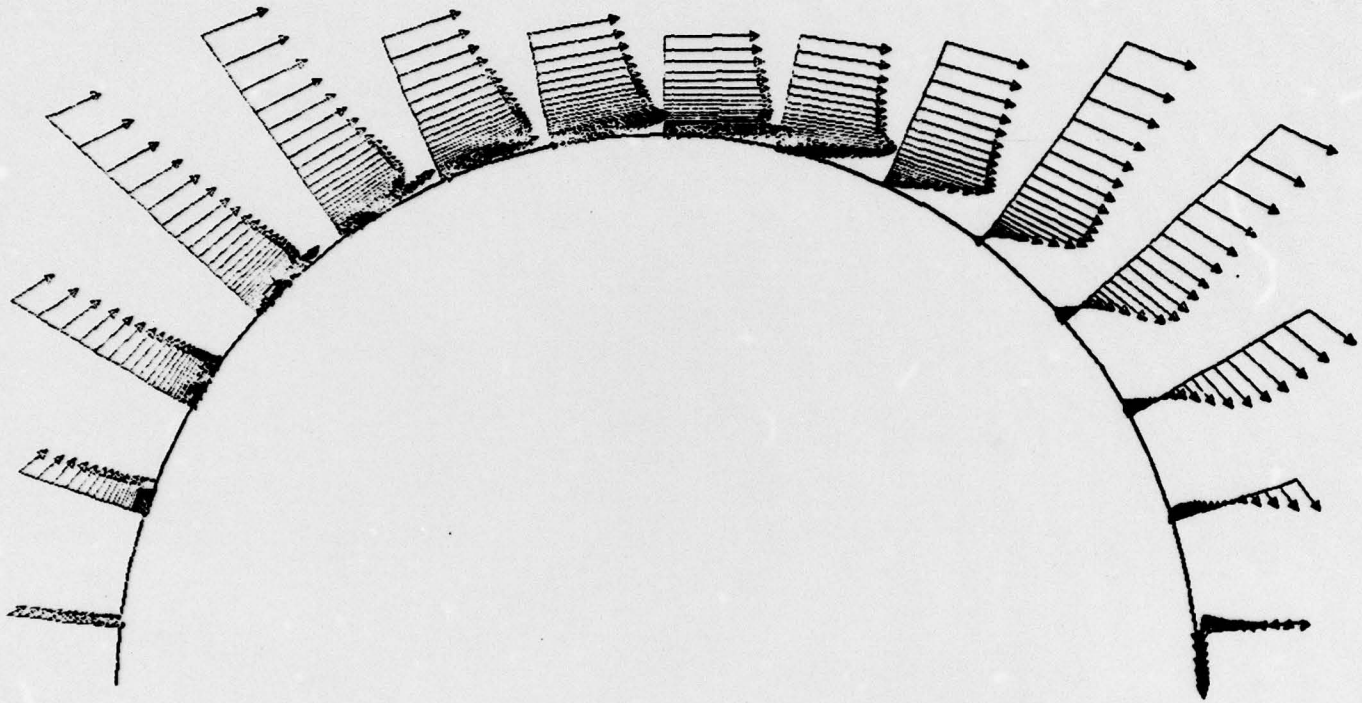

Figure 16. Velocity Vector Plot Upper Half of Field at Time 3.73.